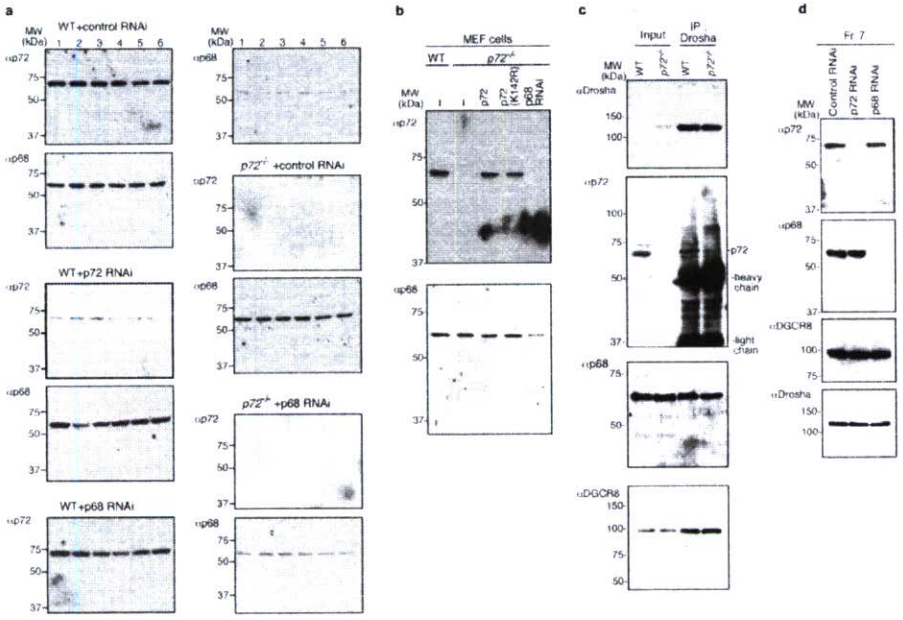

Figure S5 Selected representative full-scan images. For a, c, and d, full sized membranes were cut prior to immunoblotting according to prestained MW markers. **(a)** Images correspond to Fig. 1e. **(b)** Images correspond to Fig. 2c. **(c)** Images correspond to Fig. 4a. **(d)** Images correspond to Fig. 5f.

References

1. Sato, T. *et al.* Brain masculinization requires androgen receptor function. *Proc Natl Acad Sci U S A* **101**, 1673-8 (2004).
2. Sekine, K. *et al.* Fgf10 is essential for limb and lung formation. *Nat Genet* **21**, 138-41 (1999).
3. Shiina, H. *et al.* Premature ovarian failure in androgen receptor-deficient mice. *Proc Natl Acad Sci U S A* **103**, 224-9 (2006).
4. Kitagawa, H. *et al.* The chromatin-remodeling complex WINAC targets a nuclear receptor to promoters and is impaired in Williams syndrome. *Cell* **113**, 905-17 (2003).
5. Taganov, K.D., Boldin, M.P., Chang, K.J. & Baltimore, D. NF-kappaB-dependent induction of microRNA miR-146, an inhibitor targeted to signaling proteins of innate immune responses. *Proc Natl Acad Sci U S A* **103**, 12481-6 (2006).
6. Morgenstern, B. DIALIGN 2: improvement of the segment-to-segment approach to multiple sequence alignment. *Bioinformatics* **15**, 211-8 (1999).
7. Morgenstern, B., Frech, K., Dress, A. & Werner, T. DIALIGN: finding local similarities by multiple sequence alignment. *Bioinformatics* **14**, 290-4 (1998).

Supplementary Information

Materials and Methods

Material

For RNA ChIP primers;

pri-miR-16 (each primer number is referred for supplementary figure 3b)

1 ; Forward primer 5'-TGCTATCATAGGAGCTATGAATAAAAA-3'

Reverse primer 5'-CTTTTTCCTAAAAAGCCTTTTCTGTAAATT-3'

2 ; Forward primer 5'-AGAAAAACCGTGTAAACACACAAGT-3'

Reverse primer 5'-CAAGGACCTGATCTTCTGAAGAGAG-3'

3 ; Forward primer 5'-CATGCTAGCAAGAAGCACTTGGCCA-3'

Reverse primer 5'-TACTCTACAACTGTAATTCAATGTGTA-3'

pri-miR-214 (each primer number is referred for Figure 3)

1 ; Forward primer 5'-CGGTGTGTGGAAAATCCTGTCCCGG-3'

Reverse primer 5'-TGCCCAGTTGAGGGAAAAAATCTGG-3'

2 ; Forward primer 5'-TTGGAAGCAGCACATTGTGTCCCCA-3'

Reverse primer 5'-AGTCGATGCAGCAGACAGGGTTCAG-3'

3 ; Forward primer 5'-AGTTTAAGTCTCTGAATTATCAGTT-3'

Reverse primer 5'-AACGCCATGGACGGCTGGGGACACA-3'

4 ; Forward primer 5'-ACAACGTGCCTTATCATTTCAAAGG-3'

Reverse primer 5'-ATAATTCAGAGACTTAAACTCGAGC-3'

5 ; Forward primer 5'-TCAGAGATGCAGCTATACTATAGTA-3'

Reverse primer 5'-GAAATGATAAGGCACGTTGTCTAAA-3'

6 ; Forward primer 5'-CTGTGAAGAAAGGTTATTCTTCTTG-3'

Reverse primer 5'-AAAGGAGAGTGCAAACTCTCCTTAG-3'

7 ; Forward primer 5'-GACTTACCATACTATCCAGAGCAAG-3'

Reverse primer 5'-CAAGAAGAATAACCTTTCTTCACAG-3'

8 ; Forward primer 5'-AAATACTTGGGTGGTCCATAGGCAA-3'

Reverse primer 5'-GGGCAGAAGAGAGTAACCAGCAGCA-3'

9 ; Forward primer 5'-ATGATTTTCTTTAACTCAGATGACT-3'

Reverse primer 5'-TATGGACCACCCAAGTATTTCACTC-3'

10 ; Forward primer 5'-ATCTAAAATGTTTGAGGCTAAACTA-3'

Reverse primer 5'-TCTGAGTTAAAGAAAATCATCAAGT-3'

11 ; Forward primer 5'-GAACAATAAAATCTTTTTTGAGAAT-3'

Reverse primer 5'-TAGCCTCAAACATTTTAGATAGCAT-3'

12 ; Forward primer 5'-GCTTCTATCCCCCTTGATTAACAAG-3'

Reverse primer 5'-TTTATTGTTCATAAAACTTCTGCCT-3'

13 ; Forward primer 5'-AAAAAGAAGTTAGACGTTTGGCTTT-3'

Reverse primer 5'-TAATCAAGGGGGATAGAAGCTTATG-3'

14 ; Forward primer 5'-CTTGGGTCCTTCAGGTTTCCTTTGC-3'

Reverse primer 5'-CAAACGTCTAACTTCTTTTTAGTTC-3'

15 ; Forward primer 5'-CAGCTTTCTTTCAATGGCTGGTGGT-3'

Reverse primer 5'-CTGATTGTATCTGTCCCTGAGCAAA-3'

16 ; Forward primer 5'-TTACCCAGGCCAGACTGGCAGTTTG-3'

Reverse primer 5'-ACCACCAGCCATTGAAAGAAAGCTG-3'

17 ; Forward primer 5'-TTTTCTAAATTTACCTGTCTCTGCA-3'

Reverse primer 5'-CAATATATTCTAAAGGATCAAGTAT-3'

18 ; Forward primer 5'-TGATGTATCATTCAGCATTCTGTTG-3'

Reverse primer 5'-AGACAGGTAAATTTAGAAAATTATT-3'

19 ; Forward primer 5'-AATACACGGTAATGGCCAGTGCCAT-3'

Reverse primer 5'-GAATGCTGAATGATACATCACAAAA-3'

20 ; Forward primer 5'-TGCCTTCTCACGTAGCCCTTTCTAA-3'

Reverse primer 5'-ACTGGCCATTACCGTGTATTAAATA-3'

Construction of *p68* and *p72* targeting vectors

A 2.8-kb upstream and a 7.5-kb downstream region of *p72* genomic fragment were obtained from RPCI.23-146P10 BAC clone, to generate the targeting vector with lacZ and PGK-neo cassette to replace the translation initiation site. A 3.0-kb 5' and a 7.1-kb 3' homologous region of *p68* genomic fragment were obtained from RPCI.23-247J12 BAC clone for the targeting vector.

Generation of *p68*, and *p72* knockout mice

TT2 ES cells were electroporated with the linearized targeting vector and selected by G418. Two (p72) and three (p68) independent ES clones were isolated as homologous

recombinants by Southern blot analysis [1-3]. These ES clones were aggregated with single eight-cell embryo from CD-1 mice. Germline chimeras were bred to C57BL/6J female mice to generate heterozygous mutant F1 mice. For genotyping, high-molecular weight genomic DNA isolated from mouse tails or yolk sacs was subjected to either Southern blot analysis or PCR analysis with 5'-3' probes.

Whole-mount lacZ staining

For lacZ staining, embryos were fixed in PBS containing 1% formaldehyde, 0.2% glutaraldehyde, and 0.02% NP-40 [4]. After fixation, embryos were placed in staining buffer [44 mM HEPES (pH 7.4), 3 mM potassium ferricyanide, 15 mM NaCl, 1.3 mM $MgCl_2$, 0.5 mg/ml 5-bromo-4-chloro-3-indolyl-b-galactopyranoside (X-gal)] at room temperature.

MicroRNA microarray

Microarray experimental procedures were performed as previously described [5]. Briefly, total RNA was isolated from whole E18.5 embryos by using the *mir*Vana™ RNA Isolation kit (Ambion, Austin, TX) according to the manufacture's protocol. A flashPAGE™ fractionator System (Ambion) was used to isolate miRNA from total RNA. One hundred micrograms of total RNA was enriched for small RNA species, tailed by using the *mir*Vana™ miRNA Labeling Kit (Ambion), and fluorescently labeled by using the CyDye Mono-Reactive Dye Pack (GE Healthcare Bio-Science Corp., Piscataway, NJ, USA). Unincorporated dyes were removed with a second glass

fiber filter-based cleaning procedure. Hybridization was carried out on DNA oligonucleotide probes from the *mir*Vana™ miRNA Bioarray V2 (Ambion) containing 266 mouse miRNAs in four copies. Following hybridization, the miRNA arrays were scanned using a GenePix 4000B scanner (Axon Instruments, CA, USA). Raw data were normalized and analyzed using Array-Pro Analyzer Version 4.5 (Media Cybernetics, Inc., Silver Spring, MD, USA). Analyzed data were selected by using MicroArray Data Analysis Tool (Filgen, Inc.). Cluster analysis [6,7] was performed using Spotfire DecisionSite Functional Genomics (Spotfire Inc. Somerville, MA), applying clustering methods: Complete linkage (maximum), similarity measure: Euclidean distance and ordering Average value. Differentially expressed miRNAs were identified using one-way ANOVA followed by post hoc comparison with the Fisher's protected least significant difference test.

Whole-mount *in situ* hybridization, histology, and immunohistochemistry

Whole-mount *in situ* hybridization using digoxigenin-labelled probes was performed as previously described [4]. Each *p68* and *p72* cDNA was used as a template for riboprobe synthesis. For histological analysis, embryos and tissues were fixed with 4% paraformaldehyde in PBS and embedded in paraffin. The sections were deparaffinized, rehydrated, and stained with thionine, hematoxylin and eosin. Immunohistochemistry was performed as previously described [4].

Western blot analysis

For Western blot analysis, whole embryos and cell lysates were prepared in TNE buffer [10 mM Tris-HCl (pH 7.5), 1% NP-40, 0.15 M NaCl, 1 mM EDTA]. Proteins were separated by SDS-PAGE and Western blotted using standard conditions [4].

Immunoprecipitation

For immunoprecipitation, cells were lysed in TNE buffer. Extract from wild-type or *p72*$^{-/-}$ MEF cells were immunoprecipitated with anti-Drosha antibody and protein G sepharose. After washing, the immunoprecipitates were subjected to Western blotting analysis [4].

nature cell biology

A histone lysine methyltransferase activated by non-canonical Wnt signalling suppresses PPAR-γ transactivation

Ichiro Takada[1], Masatomo Mihara[1,3], Miyuki Suzawa[1], Fumiaki Ohtake[1,2], Shinji Kobayashi[1,2], Mamoru Igarashi[1], Min-Young Youn[1], Ken-ichi Takeyama[1], Takashi Nakamura[1,2], Yoshihiro Mezaki[1], Shinichiro Takezawa[1], Yoshiko Yogiashi[1], Hirochika Kitagawa[1], Gen Yamada[4], Shinji Takada[5], Yasuhiro Minami[6], Hiroshi Shibuya[7], Kunihiro Matsumoto[8] and Shigeaki Kato[1,2,9]

Histone modifications induced by activated signalling cascades are crucial to cell-lineage decisions. Osteoblast and adipocyte differentiation from common mesenchymal stem cells is under transcriptional control by numerous factors. Although PPAR-γ (peroxisome proliferator activated receptor-γ) has been established as a prime inducer of adipogenesis, cellular signalling factors that determine cell lineage in bone marrow remain generally unknown. Here, we show that the non-canonical Wnt pathway through CaMKII–TAK1–TAB2–NLK transcriptionally represses PPAR-γ transactivation and induces Runx2 expression, promoting osteoblastogenesis in preference to adipogenesis in bone marrow mesenchymal progenitors. Wnt-5a activates NLK (Nemo-like kinase), which in turn phosphorylates a histone methyltransferase, SETDB1 (SET domain bifurcated 1), leading to the formation of a co-repressor complex that inactivates PPAR-γ function through histone H3-K9 methylation. These findings suggest that the non-canonical Wnt signalling pathway suppresses PPAR-γ function through chromatin inactivation triggered by recruitment of a repressing histone methyltransferase, thus leading to an osteoblastic cell lineage from mesenchymal stem cells.

Histone modification on chromatin regulates transcription. Several post-translational and covalent modifications of histones have been documented, for example, methylation of lysine and arginine residues, acetylation of lysine, phosphorylation of serine and threonine residues and sumoylation of lysine. Accumulating evidence has established that hyperacetylation of histone in specific chromosomal regions generally results in activation of a given chromatin area in gene regulation, whereas hypoacetylated histones are indicators of inactive chromatin[1–3]. Other histone modifications are less predictable in how they activate chromatin; however, specific combinations of several histone modifications at certain histone residues are considered to constitute a 'histone code' that defines chromatin states for transcriptional control[1]. Among such histone modifications, lysine methylation results in unique transcriptional outcomes depending on the methylation sites, which act as docking signals for recruiting chromatin remodellers and modifiers[2–4]. Among methylated sites on mammalian chromatin, methylated H3-K9, H3-K27 and H4-K20 are considered as hallmarks of a condensed chromatin state[2]. Furthermore, H3-K9 methylation by histone lysine methyltransferase (HKMTs) triggers heterochromatin formation and transcriptionally silences euchromatic regions by recruiting heterochromatin proteins[3,4]. Reflecting the crucial roles of methylated lysines at specific sites, multiple HKMTs have been identified that recognize the same lysine residue for mono-, di- and/or tri-methylations, although the biological role of each HKMT remains elusive[4,5]. Histone modifications are altered during cell-lineage decisions, and rearrangements of histone modifications take place in response to changes in the extracellular environment[6]. However, the molecular mechanisms underlying these processes remain poorly understood.

Certain nuclear receptors (NRs) have been well researched and have been shown to integrate their ligand signals into the histone code through histone acetylation or deacetylation[7,8]. In the absence of cognate ligands, NRs are transcriptionally silent, associating with

[1]Institute of Molecular and Cellular Biosciences, University of Tokyo, Yayoi 1-1-1, Bunkyo-ku, Tokyo 113-0032, Japan. [2]ERATO, Japan Science and Technology, Honcho 4-1-8, Kawaguchi, Saitama 332-0012, Japan. [3]Department of Medicine and Bioregulatory Sciences, Institute of Health Biosciences, University of Tokushima Graduate School, Kuramoto-3, Tokushima, 770-8503, Japan. [4]Center for Animal Resources and Development (CARD), Graduate School of Medical and Pharmaceutical Sciences, Kumamoto University, Honjo 2-2-1, Kumamoto 860-0811, Japan. [5]Okazaki Institute for Integrative Bioscience, National Institutes of Natural Sciences, Okazaki, Aichi 444-8787, Japan. [6]Department of Genome Sciences, Graduate School of Medicine, Kobe University, Kobe 650-0017, Japan. [7]Department of Molecular Cell Biology, Medical Research Institute and School of Biomedical Science, Tokyo Medical and Dental University, and CREST, JST, Kanda-Surugadai, Chiyoda-ku, Tokyo 101-0062, Japan. [8]Department of Molecular Biology, Graduate School of Science, Nagoya University, Chikusa-ku, Nagoya 464-8602, Japan. [9]Correspondence should be addressed to S.K. (uskato@mail.ecc.u-tokyo.ac.jp)

Received 20 June 2007; accepted 14 September 2007; published online 21 October 2007; DOI: 10.1038/ncb1647

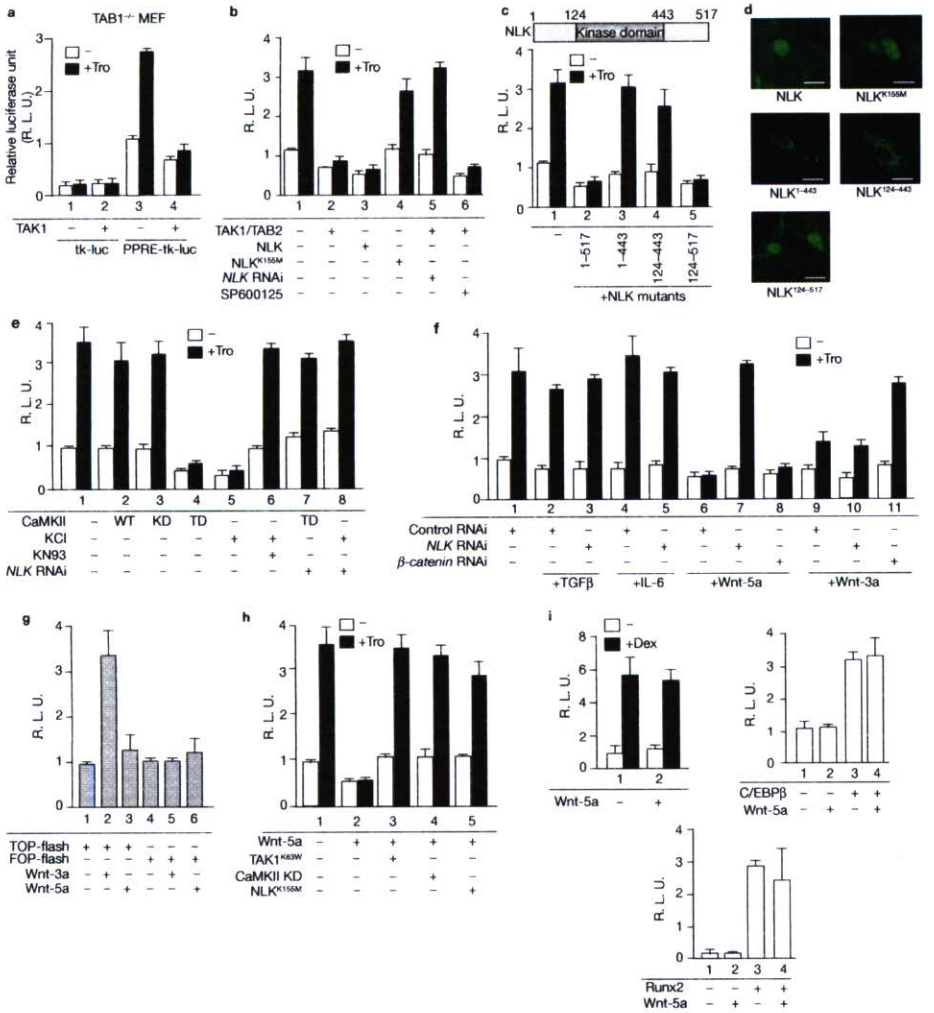

Figure 1 Wnt-5a signalling suppresses the transactivation function of PPAR-γ through CaMKII–TAK1–TAB2–NLK. (**a**) Luciferase assays in TAB1$^{-/-}$ MEF cells. After transfection with PPAR-γ, TAK1 expression vectors and acyl-CoA-PPRE-tk or tk luciferase vectors (tk-luc, thymidine-kinase-promoter–luciferase), cells were incubated with or without troglitazone (Tro). (**b**) Luciferase assays in ST2 cells transfected with PPRE-tk-luc vector and indicated expression vectors (TAK1, TAB2, PPAR-γ, NLK wild-type and kinase-negative mutants NLK^{K155M}), *NLK* RNAi or JNK inhibitor (SP600125). (**c**) Luciferase assays in ST2 cells transfected with PPRE-tk-luc vector and expression vectors of PPAR-γ and NLK deletion mutants. (**d**) ST2 cells transfected with expression vectors of GFP-fusion NLKs were scanned using a Zeiss confocal laser scanning system 510. Scale bars, 50 μm. (**e**) Luciferase assays in ST2 cells transfected with PPRE-tk-luc vector and expression vectors of PPAR-γ, CaMKII or *NLK* RNAi. WT; wild type, TD; active form, KD; kinase-dead form. Luciferase assay in ST2 cells incubated with 50 mM KCl or CaMKII inhibitor (KN93) were also performed (lane 5, 6). (**f**) Luciferase assay in ST2 cells with or without TGF-β, IL-6, Wnt-5a and Wnt-3a. *NLK* or *β-catenin* RNAi was also transfected (lane 3, 5, 7, 8, 10, 11). (**g**) Luciferase assays in ST2 cells transfected with TOP-flash or FOP-flash luc vector (TOP-flash: luc vector containing wild-type β-catenin–TCF-binding site; FOP-flash: luc vector containing mutated β-catenin–TCF-binding site) and incubated with or without Wnt-3a or Wnt-5a. (**h**) Luciferase assays in ST2 cells transfected with PPRE-tk-luc vector and PPRE-γ expression vector with or without Tro, Wnt-5a and indicated expression vectors. (**i**) Luciferase assays in ST2 cells transfected with GR (GR expression vector and GRE-luc), C/EBPβ (C/EBPβ expression vector and C/EBP-RE-tk-luc) or Runx2 (Runx2 expression vector and Runx2-RE-tk-luc). Dexamethasone (100 nM) was used to induce glucocorticoid receptor function. All error bars represent the means±s.d. of triplicate determinations (n=5×10^4 cells).

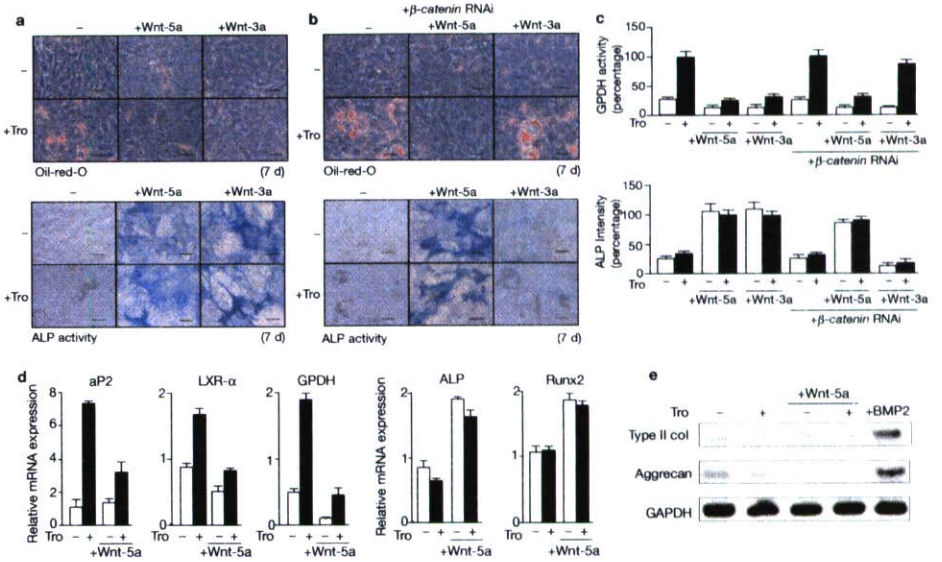

Figure 2 Wnt-5a inhibits adipogenesis and induces osteoblastogenesis in bone marrow mesenchymal stem cells. (**a**) ST2 cells incubated with or without troglitazone (Tro), Wnt-3a or Wnt-5a for 7 days were stained with Oil-Red-O (top) or for alkaline phosphatase (ALP) activity (bottom). (**b**) After transfection with β-*catenin* RNAi, ST2 cells were incubated and stained as in **a**. (**c**) Top, glycerol-3-phosphate dehydrogenase (GPDH) activities were measured using a GPDH assay kit. Bottom, measurement graph of ALP activities (A_{410}) in each cell. Error bars represent the means±s.d. of triplicate determinations. n=3×10^6 cells. (**d**) Quantitative RT–PCR of differentiation markers of adipocyte (aP2, GPDH, LXR-α) and osteoblast (Runx2 and ALP) in ST2 cells treated with/without Tro or Wnt-5a. Error bars represent the means±s.d. of triplicate determinations. n=3×10^6 cells. Expression levels were normalized for GAPDH expression. (**e**) RT–PCR analysis for differentiation markers of chondrocyte (type II collagen and aggrecan) in ST2 cells incubated with or without Wnt-5a, BMP2 and Tro was performed. Scale bars, 100 μm.

co-repressors or co-repressor complexes that often contain histone deacetylases (HDAC), which render histones hypoacetylated. Ligand binding to NRs induces clearance of such HDAC co-repressors, leading to recruitment of a co-activator or co-activator complexes in which histone acetyltransferase (HAT) activity is often detectable[7,8]. Besides ligand-induced transactivation through co-regulator switching, NRs mediate ligand-dependent and -independent transrepression through cross-talk with other intracellular signalling pathways through multiple processes of gene regulation[9].

PPAR-γ is an important NR in many biological events such as cell differentiation and cell-lineage decisions[10–12]. In particular, adipogenesis from pleiotrophic mesenchymal stem cells is primarily induced by PPAR-γ upon agonist binding[13]. However, such PPAR-γ function in adipogenesis seems to be modulated through cross-talk with other cellular signalling pathways[14]. For instance, even though bone mesenchymal stem cells are primed by PPAR-γ agonists for adipogenesis, suppression of PPAR-γ function by cytokines in progenitor cells converts the cell fate of adipogenic precursors into osteoblastic cells[15]. Osteoblastogenesis is governed by a number of regulators including Wnt peptide ligands[16–18]. Canonical and non-canonical Wnt signalling pathways are activated by multiple Wnt ligands through binding to frizzled (Fzd) plasma-membrane receptors. During activation of the canonical pathway, stabilization and nuclear translocation of the intracellular transducer β-catenin induces it to associate with members of the TCF-LEF (T-cell factor lymphoid enhancer factor) family of transcriptional factors for transcriptional activation[19]. However, downstream cascades from the non-canonical signal[20,21] remain to be uncovered and their role in mesenchymal stem-cell differentiation remains obscure.

Osteoblastogenesis is dominant over adipogenesis in the bone marrow of young animals and the cell-differentiation balance between the two cell types is usually reversed in bone marrow of elder or osteoporotic animals[18]. Therefore, we reasoned that PPAR-γ function is suppressed in the bone marrow of young animals. In the present study, we reveal that transactivation of agonist-bound PPAR-γ is repressed by a non-canonical cascade activated by Wnt-5a through the phosphorylated H3-K9 HMKT, SETDB1 (refs 22, 23) in a complex with NLK (ref. 20) and CHD7 (chromodomain helicase DNA-binding protein 7; ref. 24). This leads to a change of cell fate from adipogenesis to osteoblastogenesis of bone marrow mesenchymal stem cells even in the presence of a PPAR-γ agonist. Thus, these findings reveal a new molecular mechanism where a signal from a cell membrane receptor leads to altered histone modification and changes in gene regulation and cell-lineage decisions.

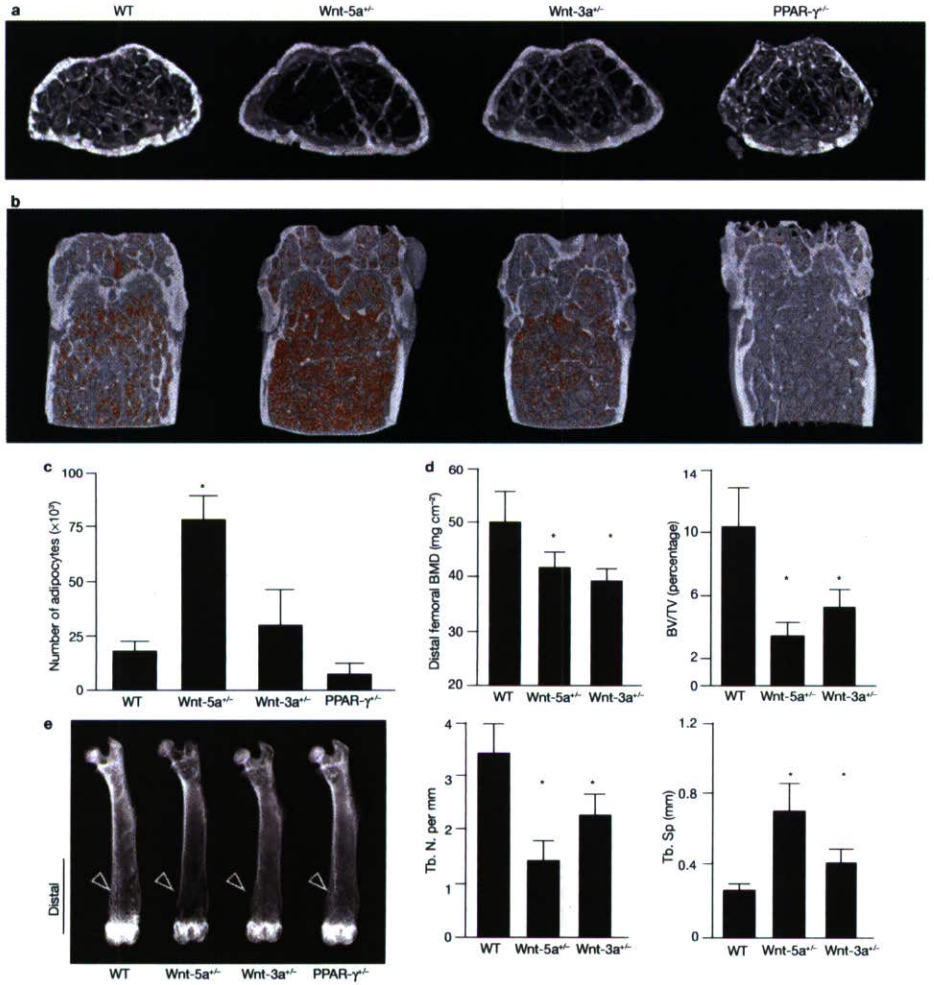

Figure 3 Bone analysis of distal femora of 18-weeks-old WT, Wnt-5a$^{+/-}$, Wnt-3a$^{+/-}$ and PPAR-γ$^{+/-}$ male mice. (**a**, **b**) Three-dimensional computational tomography images of distal femora of representative WT, Wnt-5a$^{+/-}$, Wnt-3a$^{+/-}$ and PPAR-γ$^{+/-}$ mice. In (**b**), adipocytes are displayed as orange. (**c**) The number of adipocytes was histologically measured. (**d**) Bone mineral density (BMD) of distal femora, trabecular bone volume per tissue volume (BV/TV), trabecular number (Tb. N.) and trabecular space (Tb. Sp.) were measured on the CT image. In (**c**) and (**d**), bars indicate means±s.d.(n=5 to 7 animals per genotype); Student's t-test; *, P<0.05 versus WT. (**e**) Soft x-ray image of femora from 18-week-old WT, Wnt-5a$^{+/-}$, Wnt-3a$^{+/-}$ and PPAR-γ$^{+/-}$ male mice.

RESULTS

NLK represses the transactivation function of PPAR-γ through a CaMKII–TAK1–TAB2 cascade

We previously reported that activated NF-κB transcriptionally represses activated PPAR-γ through a TAB1–TAK1-mediated (TAB1, TAK1-binding protein 1; TAK1, TGFβ-activated protein kinase 1) cascade activated by cytokines[15]. However, using TAB1$^{-/-}$ mouse embryonic fibroblast (MEF) cells[25], we unexpectedly found that TAK1 was still able to repress activated PPAR-γ in the presence of a synthetic agonist, troglitazone (Tro) (Fig. 1a). Because TAK1 serves as a mediator for other signalling cascades[20,26], we searched for a partner for TAK1 and found TAB2. By searching for downstream factors using a transient expression assay in ST2 cells (bone-marrow-derived stromal cells), a mitogen-activated protein (MAP)-kinase-like kinase, NLK, was found to replace TAK1–TAB2 and repress activated PPAR-γ (Fig. 1b). The wild-type (WT) and deletion mutants of NLK, which were potent repressors of PPAR-γ were

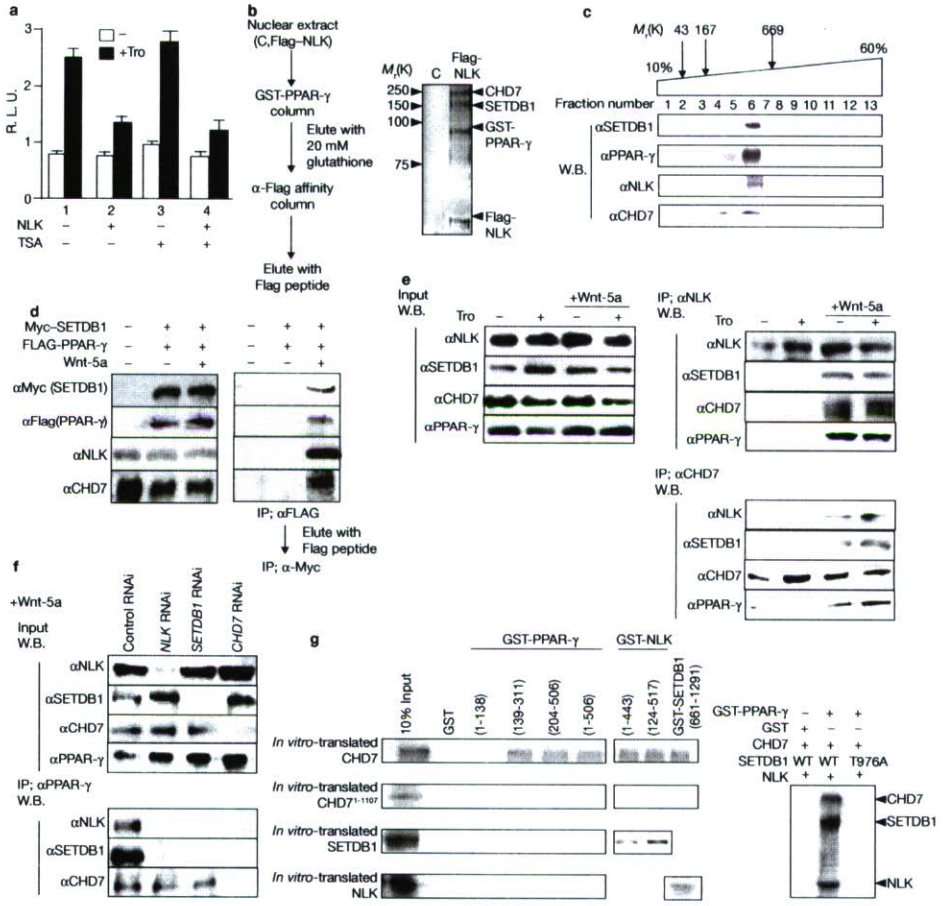

Figure 4 SETDB1 and CHD7 form a complex with PPAR-γ and NLK in a Wnt-5a-dependent manner. (**a**) Luciferase assays in ST2 cells treated with or without HDAC inhibitor (1 μM TSA) after transfection with PPAR-γ and NLK expression vectors and PPRE-tk-luc vector. Error bars represent the mean±s.d. of triplicate determinations. (**b**) Purification of the PPAR-γ–NLK complex from Flag–NLK-expressing HeLa cells using GST–PPAR-γ affinity column followed by anti-Flag immunocolumn chromatography. (**c**) Analysis of NLK–PPAR-γ complex by glycerol density gradient followed by western blotting with anti-SETDB1 and anti-CHD7 antibodies. (**d**) Two-step immunoprecipitation. ST2 cells were transfected with Flag–PPAR-γ and Myc–SETDB1 and then treated with Tro and/or Wnt-5a. Nuclear extracts were immunoprecipitated with anti-Flag and eluted with the Flag peptide. Then anti-Flag immunocomplexes were immunoprecipitated with anti-Myc and probed by western blotting with indicated antibodies. (**e**) Immunoprecipitation assay in ST2 cells after treatment with or without Tro and Wnt-5a. Nuclear extracts were immunoprecipitated with anti-NLK and anti-CHD7 antibodies. Immunoprecipitants were detected by western blotting with indicated antibodies. Uncropped images of the blots are shown in the Supplementary Information, Fig. S6a. (**f**) Immunoprecipitation assay from cells RNAi-knockdown NLK, SETDB1 or CHD7. After infection with Adeno X-RNAi against NLK, SETDB1 and CHD7 in ST2 cells, cells treated with Wnt-5a were lysed and immunoprecipitated with anti-PPAR-γ antibody. Immunocomplexes were analysed by western-blotting with indicated antibodies. (**g**) GST fusion proteins of NLK, PPAR-γ and SETDB1 were expressed in *E. coli* and used in GST pull-down assays with [^{35}S]-methionine-labelled CHD7 or CHD7$^{1-1107}$. Compared with CHD7, CHD7$^{1-1107}$ did not bind to PPAR-γ, NLK and SETDB1. When [^{35}S]-methionine-labelled CHD7, SETDB1 and NLK were incubated with GST-PPAR-γ, all components were associated with GST-PPAR-γ (right panel).

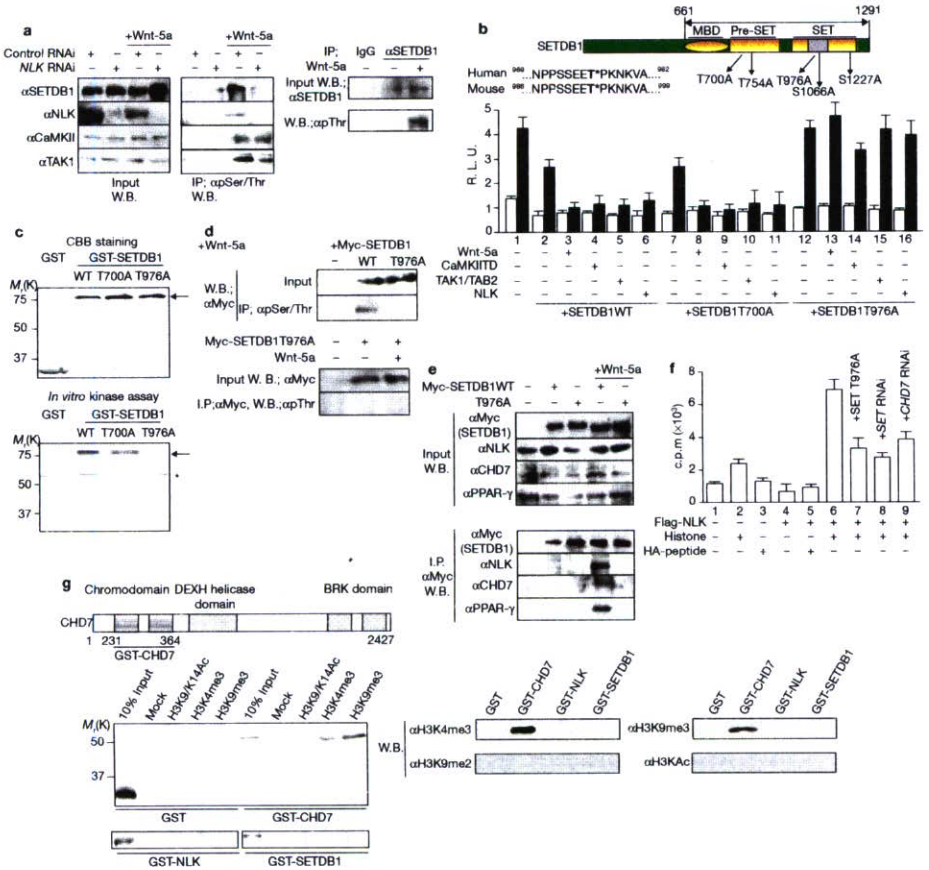

Figure 5 Phosphorylated SETDB1 forms a complex with CHD7–NLK–PPAR-γ. (**a**) Left and middle panel, lysates of ST2 cells treated with or without Wnt-5a and transfected with control or *NLK* RNAi were applied to anti-Ser–Thr phosphorylation columns, then probed with indicated antibodies. Uncropped images of the blots are shown in the Supplementary Information, Fig. S6b. Right panel, lysates of ST2 cells treated with or without Wnt-5a were immunoprecipitated by IgG or anti-SETDB1 and then probed by anti-phosphothreonine (pThr). (**b**) Predicted phosphorylation sites of SETDB1 (661–1291). Thr976 is conserved between humans and mice. Luciferase assays in ST2 cells transfected with PPRE-tk-luc vector, PPAR-γ expression vector and indicated expression vectors were performed. Error bars represent the mean±s.d. of triplicate determinations. $n=5\times10^4$ cells. (**c**) NLK phosphorylates GST–SETDB1 *in vitro*. Upper panels, GST-fusion SETDB1 (WT, T976A and T700A) proteins were stained with CBB (upper panel, arrow indicates GST–SETDB1). Lower panels, the *in vitro* kinase assay was performed as described in the methods. (Arrow indicates GST–SETDB1, and the asterisk indicates self-phosphorylated NLK.) (**d**) SETDB1 T976A is not phosphorylated *in vivo*. Upper panel, after transfection with the indicated expression vector, immunoprecipitation with anti-Ser–Thr phosphorylation columns and western blotting was performed. Lower panel, after transfection with Myc–SETDB1T976A expression vector, cell extracts were immunoprecipitated with anti-Myc and probed with anti-phosphothreonine. (**e**) Immunoprecipitation assay in ST2 cells. After transfection with Myc–SETDB1 or SETDB1 T976A expression vector, immunoprecipitation with anti-Myc sepharose and western blotting were performed using the indicated antibodies. (**f**) NLK immunocomplexes possess histone methyltransferase activity. After transfection with Flag–NLK expression vector and the indicated vector and RNAi, in ST2 cells and immunoprecipitation with anti-Flag column, HMT assays were performed. Error bars represent the means±s.d. of triplicate determinations. $n=5\times10^4$ cells. (**g**) Upper panel, the peptide pull-down assay was performed using purified GST and GST-fused proteins with various modified H3 peptides (1–21 a.a.) indicated on top. Bound proteins were analysed by SDS-PAGE and silver staining. Lower panels, histone-binding assays were performed using HeLa histone extract and GST, GST–CHD7, –NLK and –SETDB1. Bound proteins were analysed by SDS-PAGE and western blotting. Uncropped images of the blots are shown in Supplementary Information, Fig. S6c.

localized in the nucleus (Fig. 1c, d). Although a kinase-negative mutant (NLK^{K155M}) was located in the nucleus (Fig. 1d), this mutant lost transrepressive activity for PPAR-γ (Fig. 1b).

CaMKII (calcium/calmodulin-dependent protein kinase II) is an upstream factor of TAK1–TAB2 that activates NLK for its repressive activity[20]. Treatment with KC1, which activates CaMKII, was effective in repressing PPAR-γ function (Fig. 1e). A constitutively kinase-dead form of CaMKII (CaMKII KD) and the CaMKII inhibitor KN93 abrogated the suppressive activity of NLK for PPAR-γ (Fig. 1e). Through investigating membrane-receptor ligand candidates that activate NLK in ST2 cells, we found that Wnt-5a mediated the suppressive function of NLK (Fig. 1f). However, Wnt-5a action was not abrogated by knockdown of β-catenin (Fig. 1f) and, unlike Wnt-3a, Wnt-5a did not activate the TCF-LEF-mediated canonical cascade (Fig. 1g).

An activated non-canonical Wnt cascade attenuates adipogenesis through repression of PPAR-γ activity

Expression of Wnt ligands and their receptors was tested in ST2 cells. ST2 cells are derived from mouse bone marrow stromal cells and differentiate into either adipocytes through PPAR-γ activation or osteoblasts if induced by several cytokines[15]. We observed that Wnt-5a and several frizzled receptor genes are expressed at significant levels in ST2 cells as well as in mouse bone marrow cell primary culture (data not shown).

Wnt-5a, but not the canonical Wnt ligand Wnt-3a, was capable of repressing PPAR-γ function through NLK on synthetic (Fig. 1f) as well as natural PPAR-γ target gene promoters (see Supplementary Information, Fig. S1a). $TAK1^{K63W}$ (a kinase-dead mutant of MAPKKK), CaMKII KN as well as NLK^{K155M} abrogated Wnt-5a-induced suppression of PPAR-γ (Fig. 1h). Furthermore, knockdown of NLK (see Supplementary Information, Fig. S2) abolished the effect of Wnt-5a, CaMKII and TAK1–TAB2 (Fig. 1b, e, f). Transactivation functions of adipogenic (CCAAT/enhancer binding protien (C/EBPβ), glucocorticoid (GR)) or osteoblastogenic (Runx2) transcriptional factors were not modulated by Wnt-5a treatment (Fig. 1i). It is notable that the activated non-canonical Wnt signalling by Wnt-5a lowered the basal activity of the tested PPAR-γ target gene promoters (see Fig. 1h for instance). Interestingly, PPAR-γ phosphorylation mutants (PPAR-γ S8A, S112A and S8A-S112A), which have been reported to be insensitive to MAPK (ERK)-induced suppression[14], remained susceptible to the suppressive action of NLK (see Supplementary Information, Fig. S1b).

Wnt-5a has been identified as a potential genetic determinant of diet-induced obesity[27] and so we examined the effect of Wnt-5a on ST2 cell differentiation. Treatment with Tro induced adipogenesis, lipid accumulation and glycerol-3-phosphate dehydrogenase (GPDH) activity (Fig. 2a, c) as reported previously[15,28]. Under these conditions, Wnt-5a seemed to mediate transdifferentiation of adipo-progenitors into osteoblastic cells expressing alkaline phosphatase (ALP) (Fig. 2a, c), as reflected by expression of markers of mature adipocytes (GPDH, aP2 and LXR-α) and osteoblasts (ALP and Runx2) (Fig. 2d and Supplementary Information, Fig. S1c), but not chondrocyte-specific markers (type II collagen and aggrecan) (Fig. 2e). Knockdown of β-catenin by RNA interference (RNAi) did not abrogate Wnt-5a-induced adipogenesis inhibition (Fig. 2b, c). Again, this supports the involvement of the non-canonical Wnt cascade activated by Wnt-5a in promoting osteoblastogenesis through attenuating adipogenesis with induction of Runx2, a critical osteoblastogenic transcription factor (Fig. 2d and Supplementary Information, Fig. S1c). Although TAZ (transcriptional co-activator with PDZ-binding motif) has recently been identified as an osteoblastogenic factor of mesenchymal stem-cell differentiation by repressing PPAR-γ function[29], TAZ seemed to be independent from the mechanism of Wnt-5a-induced suppression of the transactivation function of PPAR-γ (see Supplementary Information, Fig. S3a), and also independent from adipogenesis inhibition (see Supplementary Information, Fig. S3b). Together with the observation that *TAZ* gene expression is unaltered by Wnt-5a treatment (see Supplementary Information, Fig. S3c), we assume that the TAZ-mediated cascade does not converge with that of Wnt-5a in the differentiation of mesenchymal stem cells. Thus, activated PPAR-γ seems to potentiate cytodifferentiation of mesenchymal stem cells into adipo- or osteo-progenitors.

Wnt-5a haploinsufficiency in mice induces bone loss with enhanced adipogenesis in bone marrow

As expected from the physiological effect of PPAR-γ on adipogenesis from mesenchymal stem cells in bone marrow[30], haploinsufficiency of PPAR-γ in mice ($PPAR\text{-}\gamma^{+/-}$) resulted in a reduction of adipocytes in bone marrow (Fig. 3b, c). Moreover, as expected from *in vitro* observations, bone mass increase, presumably because of increased osteoblastogenesis from bone marrow stem cells, was observed in $PPAR\text{-}\gamma^{+/-}$ male mice[31] (Fig. 3a, b, e). By contrast, $Wnt\text{-}3a^{+/-}$ males[32] exhibited bone loss (Fig. 3a, b, d, e), consistent with previous reports that canonical Wnt signalling is responsible for bone formation through stimulating osteoblastogenesis[33–35]. However, unlike $PPAR\text{-}\gamma^{+/-}$ mice, adipogenesis seemed unaffected in $Wnt\text{-}3a^{+/-}$ mice (Fig. 3b), suggesting that canonical Wnt signalling is unlikely to attenuate adipogenesis from adipo- or osteo-progenitor cells.

Supporting *in vitro* observations of $Wnt\text{-}5a^{+/-}$ mice[36] showed a clear bone-loss phenotype, with decreased trabecular bone mass (Fig. 3d, and see arrow heads of Fig. 3e). Presumably, this was caused by reduced osteoblastogenesis as shown in the femur (Fig. 3a), which shows significantly elevated number of adipocytes in bone marrow (Fig. 3b, c) when compared with wild-type littermates. Taken together, these findings confirm that Wnt-5a potentiates the cell-lineage decision of bone marrow mesenchymal stem cells into osteoblasts, presumably through the non-canonical Wnt signalling pathway.

NLK activated by Wnt-5a forms a complex with a HKMT

We then tested whether NLK-induced suppression of PPAR-γ function was linked to HDAC using the HDAC inhibitor, tricostatin A (TSA). However, TSA was unable to reverse NLK-mediated suppression of PPAR-γ function in ST2 cells (Fig. 4a). No alteration in PPAR-γ protein turnover was detected even when NLK was overexpressed (see Supplementary Information, Fig. S4a). Considering that NLK is a downstream factor of activated Wnt-5a (ref. 20), we reasoned that NLK might associate with unknown co-regulators to suppress PPAR-γ function. We therefore biochemically purified NLK-containing complexes from nuclear extracts of KCl-treated HeLa cells expressing Flag-tagged NLK by two-step purification[37,38] (Fig. 4b). We identified an NLK–nuclear-protein complex with a molecular weight of around 400–500 kDa by using glycerol gradient centrifugation fractionation (Fig. 4c). By MALDI-TOF mass spectrometric analysis of the other two complex components, two proteins (220 kDa and 170 kDa) were identified. The 220-kDa band was a DEXH-box and CHD-domain-containing ATPase protein, CHD7

(ref. 24). The 170-kDa band was an HKMT (SETDB1) that suppresses transcription through histone H3 methylation at K9 (refs 22, 23). We confirmed the formation of these complexes by a two-step immunoprecipitation assay (Fig. 4d) and association of endogenous NLK, SETDB1 and CHD7 in a complex with PPAR-γ was only detectable after treatment with Wnt-5a in ST2 cells (Fig. 4e). This Wnt-5a-induced association was abrogated when NLK, SETDB or CHD7 was knocked down by RNAi (Fig. 4f). In a GST pull-down assay, CHD7 seemed to be able to physically interact with NLK, SETDB1 and PPAR-γ, whereas PPAR-γ did not interact with SETDB1 (Fig. 4g). However, PPAR-γ seemed to associate with SETDB1 in the presence of CHD7 (Fig. 4g; lower panel).

SETDB1 T976A phosphorylation by NLK is a prerequisite for HKMT activity and transrepression of PPAR-γ

We hypothesized that Wnt-5a-activated NLK phosphorylates SETDB1, because SETDB1 harbours several putative phosphorylation sites that could be NLK substrates (Fig. 5b). Using an anti-phosphorylated Ser–Thr antibody column, endogenous SETDB1 was found to be phosphorylated in a Wnt-5a-dependent manner (Fig. 5a). Wnt-5a-induced phosphorylation and repressive action on PPAR-γ was tested using SETDB1 deletion mutants (see Supplementary Information Fig. S4b). The mapped carboxy-terminal domain contains putative Thr–Ser phosphorylation site residues, and these were mutated to alanine (T700A, T754A, T976A, S1066A and S1277A; Fig. 5b). Among the five tested SETDB1 point mutants, only the T976A mutant was found to be deficient in SETDB1 repressive action (Fig. 5b) and was not phosphorylated by NLK either *in vivo* or *in vitro* (Fig. 5c, d). Interestingly, as a reflection of the importance of Thr976 phosphorylation for SETDB1 function, the region around Thr976 is highly conserved between human and mouse SETDB1 despite having only about 75% homology in adjacent regions (Fig. 5b). Significantly, Wnt-5a-induced complex formation of NLK–CHD7 with SETDB1 and PPAR-γ was abrogated by the T976A point mutation (Fig. 5e). The expected activity of the SETDB1 histone methyltransferase was detected in the NLK complex from Wnt-5a-treated ST2 cells (Fig. 5f). However, knockdown of either SETDB1 or CHD7 reduced the histone methyltransferase activity of the NLK complex (Fig. 5f), suggesting that SETDB1 requires assembly with NLK and CHD7 as a complex. Reflecting the presence of two chromodomains[39] in CHD7, CHD7 demonstrated physical interactions with tri-methylated H3-K4 and H3-K9 in a peptide pull-down assay and a histone-binding assay with semi-purified histones from HeLa cells (Fig. 5g). However, such preferential and significant interactions were not detected for acetylated H3.

Wnt-5a-induced H3-K9 methylation represses PPAR-γ-dependent activation of PPAR-γ target gene promoters

We then performed a chromatin immunoprecipitation (ChIP) analysis of endogenous transcriptional factors and histone modifications at the PPAR-γ binding site (PPRE) of the aP2 gene promoter[13]. Tro treatment induced recruitment of known PPAR-γ co-activator SRC-1 and co-repressor N-CoR (Fig. 6a). Treatment with Wnt-5a for 6 h in the presence of Tro induced recruitment of NLK, CHD7 and SETDB1 to the proximal PPRE region, but not to the other distal region on the aP2 gene promoter. Furthermore, consistent with SETDB1 recruitment, an increase in histone di- and tri-methylation at histone H3-K9 was observed together with hypoacetylation of histone H3 (Fig. 6a). Similar findings were also observed with the other PPAR-γ target gene (LXR-α) promoter (see Supplementary Information, Fig. S5b). Such coordinated histone modification to inactivate chromatin was more evident when ST2 cells were treated with Wnt-5a for 7 d to induce osteoblastogenesis (Fig. 6b). In comparison, histone H3-K9 on the Runx2 promoter was highly acetylated, and recruitment of neither PPAR-γ nor SETDB1 was seen in the same cells treated with Wnt-5a (Fig. 6c). These observations suggested that the Runx2 gene promoter is transcriptionally active in the presence of Wnt-5a, consistent with induction of the *Runx2* gene during Wnt-5a-induced osteoblastogenesis (Fig. 2d and see Supplementary Information, Fig. S1c).

Wnt-5-induced osteoblastogenesis from adipo- or osteo-progenitor cells requires NLK, SETDB1 and CHD7

With reference to these findings, we observed that overexpression of either NLK or SETDB1 was able to induce osteoblastogenesis rather than adipogenesis in ST2 cells (Fig. 7a, b; see Supplementary Information Fig. S2). Conversely, overexpression of an NLK mutant (NLK-KD) and SETDB1 mutants (SETDB1 T976A and ΔSET) and knockdown of NLK, SETDB1 or CHD7 induced adipogenesis rather than osteoblastogenesis even in the presence of Wnt-5a (Fig. 7a–d). Furthermore, these knockdowns abrogated the Wnt-5a-induced H3-K9 methylation and subsequent histone modification in the aP2 gene promoter (compare Fig. 6b with 7e).

DISCUSSION

Activated PPAR-γ is remarkably potent in cytodifferentiation, and several co-regulators of PPAR-γ, and cross-regulation by other cellular signalling pathways, have been previously described[10–12]. In particular, during PPAR-γ agonist-induced adipogenesis from bone marrow mesenchymal stem cells, activated PPAR-γ seems to function at multiple steps of the cytodifferentiation process. This is evident because bone marrow mesenchymal stem cells are pleiotropic and can differentiate into osteoblasts, chondrocytes or myoblasts depending on the activities of cell-lineage determinants[17].

In this study, we have found that Wnt-5a induces osteoblastogenesis through attenuating PPAR-γ-induced adipogenesis in mesenchymal stem cells of bone marrow. Wnt-5a activated a non-canonical Wnt signalling cascade mediated through CaMKII–TAK1–TAB2–NLK, but did not trigger the β-catenin–TCF canonical Wnt signalling pathway. Wnt signalling pathways have previously been described as being able to cross-talk with signalling pathways of certain NRs[40,41], and the pivotal roles of such cross-talk in cell-fate decisions have recently been verified in *Caenorhabditis elegans*[42]. This would suggest that such cross-regulation is conserved in metazoans. However, unlike the non-canonical Wnt cascade presented here, the canonical pathway mediated through β-catenin–TCF is known to co-activate the transactivation function of activated NRs including PPAR-γ (refs 40, 41). Thus, it is likely that Wnt ligands, in a positive or negative manner, modulate the functions of NRs in transcriptional control, depending on their specific downstream signalling cascades.

Osteoblastogenesis was induced by Wnt-5a in ST2 cells even in the presence of a PPAR-γ agonist. Supporting these *in vitro* observations, Wnt-5a$^{+/-}$ mice exhibited a reduction in bone mass presumably because of a reduced number of osteoblasts whereas increased numbers of adipocytes were seen in the bone marrow (Fig. 3b). Bone mass decrease was also detectable in Wnt-3a$^{+/-}$ mice (Fig. 3a, b, d, e) presumably owing to impaired canonical Wnt signalling, consistent with recent reports that the canonical Wnt cascade through LRP5–β-catenin (LRP5: low-density lipoprotein receptor-related protein 5) is indispensable for osteoblastogenesis[33–35]. Wnt signalling thus seems to contribute to osteoblastogenesis from bone marrow mesenchymal cells through both canonical and non-canonical cascades. However, in terms of preventing the adipogenesis cell-lineage decision, only non-canonical Wnt signalling plays a significant part in bone marrow development.

It was recently reported that TAB2 in macrophage cells activated by the IL-1 signalling cascade prevents clearance of an HDAC co-repressor complex from ligand-bound sex steroid receptors, thus maintaining a transcriptionally repressive state of the steroid receptor[43]. In the present study, interestingly, an HDAC inhibitor (TSA) failed to abrogate the Wnt-5a effect on PPAR-γ transrepression (Fig. 4a), and, consistent with this finding, HDAC3 and N-CoR were not detected 6 h after Wnt-5a treatment (Fig. 6a). However, before Wnt-5a treatment in the absence of Tro, HDAC3 and N-CoR were associated with the promoter (Fig. 6a and Supplementary Information, Fig. S5a), and Wnt-5a seemed to induce clearance of the N-CoR-HDAC complex and block SRC-1 recruitment even in the presence of Tro. These findings clearly suggest that the

Figure 6 Wnt-5a-dependent recruitment of NLK containing corepressor complex. (**a**, **b**) Chromatin immunoprecipitation analysis of the aP2 promoter in ST2 cells treated with or without Troglitazone and Wnt-5a for 6 h (**a**) or 7days (**b**) was performed using indicated antibodies. (**c**) ChIP analysis of Runx2 promoter in ST2 cells. ST2 cells were treated with or without Wnt-5a, and ChIP analysis was performed using indicated antibodies.

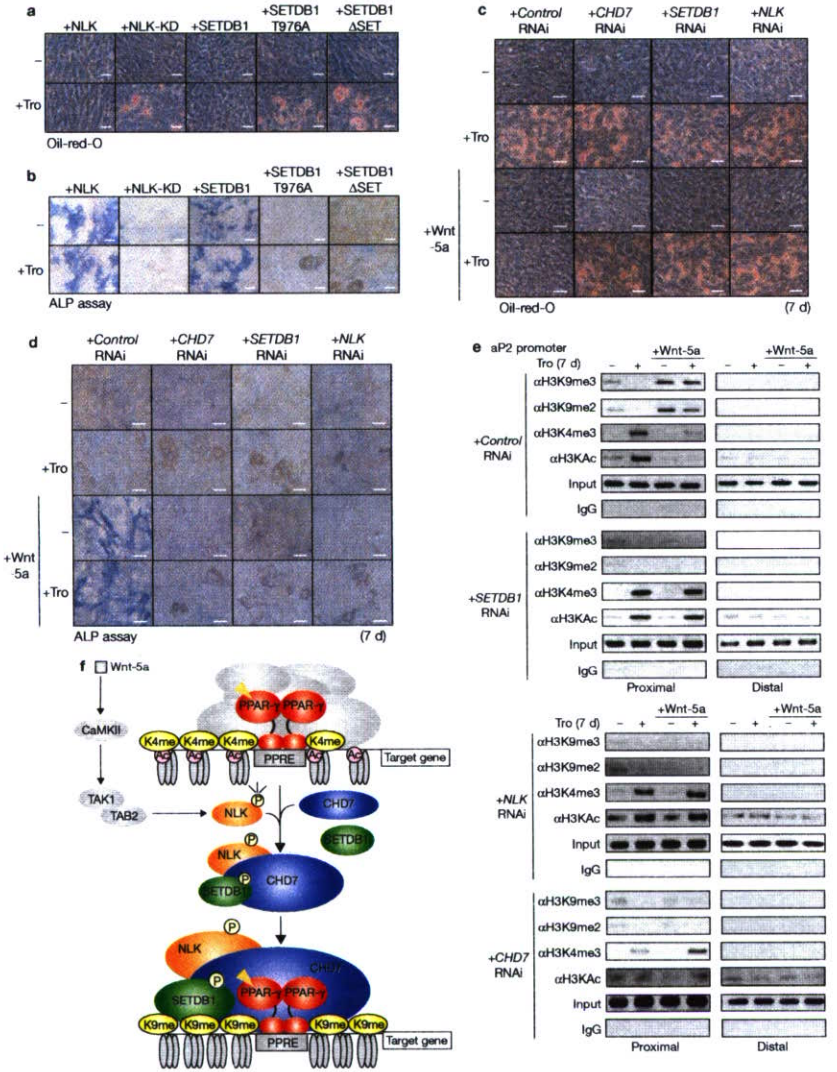

Figure 7 *NLK*, *SETDB1* and *CHD7* RNAi abrogated Wnt-5a-dependent differentiation and recruitment of modified H3. (**a**, **b**) ST2 cells overexpressed with NLK or SETDB1 mutants (NLK-KN, SETDB1T976A or SETDB1ΔSET) were incubated for 7 d, then stained with Oil-red-O (**a**) and ALP assay (**b**). Scale bars, 100 μm (**c**, **d**) *SETDB1* and *CHD7* RNAi abrogated the Wnt-5a dependent inhibition of adipogenesis. Control, *SETDB1* or *CHD7* RNAi adenovirus was infected in ST2 cells and stained with Oil-Red-O (**c**) or by ALP assay (**d**). (**e**) Chromatin immunoprecipitation analysis on aP2 promoter in ST2 cells expressing *SETDB1*, *NLK* or *CHD7* RNAi. (**f**) A mechanistic model for Wnt-5a dependent suppression of PPAR-γ function. Activated NLK through Wnt-5a-CaMKII–TAK1–TAB2 phosphorylates SETDB1. Then phosphorylated SETDB1 associates with CHD7 and act as a repressor for PPAR-γ transactivation function. CaMKII, calmodulin kinase II; PPRE, PPAR-response element; K4me, tri-methylated histone H3K4; K9me, tri-methylated histone H3K9; grey square, Wnt-5a.

transrepression of PPAR-γ by Wnt-5a mediates a histone-inactivating mechanism other than histone deacetylation by a HDAC co-repressor complex. We identified an HKMT, SETDB1, as an interacting partner of activated NLK by Wnt-5a by a biochemical approach. SETDB1 seems to form a complex with CHD7 and phosphorylated NLK. However, under our purification conditions, known SETDB1 partners such as human ATFa-associated modulator (hAM) were undetectable[23]. The SETDB1 complex associated with PPAR-γ to methylate H3-K9 in the PPAR-γ target gene promoters leading to inactivation of gene expression through histone-inactivating modifications. Thus, this complex is presumed to be a new type of HKMT co-repressor complex for nuclear receptors in terms of signalling dependency. These findings are supported by a recent report that several H3-K9 HKMTs serve as co-repressors for ligand-bound nuclear receptors[44,45], although signal-induced recruitment of HKMT to nuclear receptors was not reported. In this respect, it is notable in a previous report that repression of A-Myb by activated NLK through the Wnt-1–TAK1–TAB1–HIPK2 axis was mediated by an as yet unidentified HKMT[46]. SETDB1 might be a nuclear target activated by signalling of cell-membrane receptors to co-repress several classes of transcriptional factors.

SETDB1 is shown here to be integrated into a complex through phosphorylation by activated NLK, and it then serves as a co-repressor complex component with CHD7, a platform component. Interestingly, the HKMT activity of SETDB1 required complex formation induced by the non-canonical cascade. Given that hAM is reportedly a crucial partner for forming a complex with SETDB1 that has HKMT activity and can transcriptionally repress[23], SETDB1 might be a catalytic subunit that is fully functional only when integrated into distinct protein complexes. Co-activators and co-activator complexes are required for ligand-induced transactivation of PPAR-γ, but the SETDB1–NLK–CHD7 complex seems to attenuate recruitment of such co-activators to ligand-bound PPAR-γ. In this regard, CHD7 seems to be a docking component in the complex for PPAR-γ, considering the observed interaction of CHD7 with PPAR-γ *in vitro*. Moreover, because CHD7 harbours two chromodomains that selectively recognize and preferentially bind to methylated histone lysines[39], CHD7 could also anchor this complex to specific chromosomal regions. In fact, CHD7 was revealed to selectively interact with methylated H3-K4 and H3-K9, but not acetylated histones (Fig. 5g), implicating multiple roles of CHD7 in transcriptional repression. CHD7 may target the SETDB1 complex to transcriptionally active regions through interacting with methylated H3-K4, and then SETDB1 might initiate H3-K9 methylation in the PPAR-γ target gene promoters (Fig. 7f). At the present stage, it remains unclear whether methylated H3-K4 is an initial docking signal for recruiting the SETDB1 complex or whether this complex is first recruited to PPAR-γ. Furthermore, at later stages of the repression process, through stable retention of the SETDB1 complex through interaction of CHD7 with tri-methylated H3-K9 at the promoters, the SETDB1 complex might trigger heterochromatinization from transcriptionally silent euchromatin. In this respect, CHD7, but not SETDB1, might define the target specificity of the PPAR-γ target promoters by acting as an anchor to chromatin. Likewise, other silencing factors such as DNA methyltransferase and methyl-binding protein may be recruited through CHD7 to the target promoters for stable transrepression.

For every histone modification at a specific residue, multiple histone-modifying enzymes have been identified as recognizing the same histone residue. As recent findings have shown that histone-modifying enzymes often form complexes as enzymatically functional units[45], it is conceivable that complex components enable enzymes to specifically recognize histone residues as substrates and serve as regulatory subunits that integrate with intracellular signalling. Thus, the combination of histone-modifying enzymes with their complex partners might be prerequisite for their specific roles in gene regulation at the chromatin level. □

METHODS

Plasmid construction. Expression vectors of full-length PPAR-γ, PPAR-γ mutants (S8A, S112A and S8A-S112A), TAK1, TAK1^{K63W}, C/EBPβ, GR and acyl-CoA-PPRE-tk, GRE-tk, C/EBP-RE-tk luciferase reporter vectors, GST-fusion PPAR-γs (amino acids 1–506, 1–138, 139–311, 204–506) were constructed as previously described[15]. Expression vectors of CaMKII (WT, KN and TD) and Flag–NLK and Flag–NLK^{K155M} were constructed as previously described[20]. Deletion mutants of NLK (amino acids 1–443, 124–443, 124–517) and GFP-fusion mutants of NLK were amplified by polymerase chain reaction (PCR) and cloned into pcDNA3 (Invitrogen, Carlsbad, CA) and pGEX4T-1 (Amersham, Piscataway, NJ). SETDB1 and CHD7 were cloned by PCR and inserted into pcDNA3. SETDB1ΔSET(amino acid 1–660) was cloned by PCR and inserted into pcDNA3 and SETDB1 point mutants were generated by PCR-based mutagenesis using pcDNA3-SETDB1 as a template. For GST-fusion CHD7, CHD7 constructs (amino acids 231–364) were cloned by PCR and inserted into pGEX4T-1. The expression vector of Runx2 and Runx2-RE-tk luciferase reporter vector have been previously described[17]. For luciferase assays, the DNA sequence for RNAi against β-*catenin* and *NLK* were as follows: β-*catenin*, CACGCAAGAGCAA GTAGCTGATATT; *NLK*, GAAATATCTCCATTCAGCTGGCATT.

Cell culture, Wnt-5a treatment, transfection and luciferase assays. ST2 cells were cultured and examined using Oil-red-O staining and alkaline phosphatase assays as described previously[15]. For differentiation assays, cells were treated with or without 1 μM of Tro or 50 ng ml^{-1} of recombinant Wnt-5a (R&D Systems, Minneapolis, MN) for 7 d. GPDH activity was measured using the GPDH activity measurement kit (Takara, Ohtsu, Japan). The luciferase reporter assay was performed as previously described[15].

Animal preparation. The generation of Wnt-5a$^{+/-}$, Wnt-3a$^{+/-}$ and PPAR-γ$^{+/-}$ gene-target mice was previously described[32,36,47]. These mice were crossed with C57BL6 over five generations. All experiments were performed on male mice at 18 weeks of age, and mice littermates were fed a standard diet. All mice were maintained according to the protocol approved by the Animal Care and Use Committee of the University of Tokyo.

Analysis of skeletal morphology and μ-QCT imaging. The femora were collected from 18-week old WT, Wnt-5a$^{+/-}$, Wnt-3a$^{+/-}$ and PPAR-γ$^{+/-}$ mice and fixed in 70% ethanol. Femoral bone mineral densities were determined by dual-energy X-ray absorptiometry (DCS-600EX-III, ALOKA, Tokyo, Japan). Femur bone radiographs were obtained using a soft X-ray apparatus (TRS-1005, SOFTRON, Yokohama, Japan). Histomorphometric analysis for measurement of BV/TV, trabecular number and space was conducted by the Bone Analysis Service at Kureha Special Laboratory (Tokyo, Japan). For micro-quantitative computed tomography (μ-QCT) imaging, soft tissue was meticulously removed and placed in a special polycarbonate specimen tube filled with distilled water and scanned by ScanXmate-A100S40 (Comscan techno, Yokohama, Japan). Data sets with isotropic 8.6 μm voxel spacing were acquired at 0.45° steps over a total rotation of 360° at 80 kVp. Images were reconstructed into three-dimensional volumes using true Feldkamp reconstruction with 10-bit grey levels. To determine adipocytes in bone, an upper and lower pixel intensity threshold (LUT) was chosen (110–160; adipocytes). The highlighting tool was used to select individual adipose depots for pixel counting.

RNA analysis. Total cellular RNA was isolated from ST2 cells by ISOGEN (Wako, Tokyo, Japan), and quantitative reverse transcribed PCR (RT–PCR) was performed on a TP800 sequence detector (Takara, Ohtsu, Japan). The primers used are described in the Supplementary Information. For RT–PCR analysis, RT reaction was performed using SuperScript III (Invitrogen, Carlsbad, CA), and aggrecan (amino acids 150–290) and type II collagen (amino acids 1395–1451) were amplified by PCR.

Immunoprecipitation and ChIP analysis. The immunoprecipitation assay was performed as previously described[48]. For the ChIP assay, ST2 cells were incubated with or without Tro or Wnt-5a. We used the ChIP Assay Kit (Upstate, Lake Placid, NY) with antibodies against acetylated histone H3, trimethylK9H3 (Upstate), PPAR-γ, NLK (Santa Cruz Biotechnology, Santa Cruz, CA) or SETDB1 (Axxora, San Diego, CA). Antibody against CHD7 was produced by Asahi Technoglass (Funabashi, Japan). For PCR, we used the following primer pairs: 5′-AGTTC ACTAGTGGAAGTGTCACAGC-3′ (−5340 to −5315) and 5′-CTAGAAACAG ACACTGGAACCACTCT-3′ (−4800 to −4775) for aP2 gene promoter region at PPRE, and 5′-ACAGGCCTGCACAGAGGACGTTTCC-3′ (−7763 to −7739) and 5′-CATCATTTGCTATAAGTTGATTAGG-3′ (−7464 to −7439) for aP2 gene distal region. For amplification of Runx2 promoter by PCR, we used the primer pairs 5′-GGTAGAGAAGAGAGATGAAAAAGCAGAGG-3′ (−546 to −518) and 5′-GGTGTTCCTCTGTCTCTCCTTCCCT-3′ (−268 to −244) for the *Runx2* gene promoter region[49], and 5′-GCTACAATGTCGATATTCCTC-3′(−3939 to −3919) and 5′-GCATATCTGGTTGTGAGTAC-3′ (−3568 to −3549) for the *Runx2* gene distal region. Optimal PCR conditions for semi-quantitative measurement were 27 cycles of 30 s at 96 °C, 45 s at 56 °C, and 1 min at 72 °C. PCR products were visualized on 2% agarose-Tris-Acetate-EDTA (TAE) gels.

***In vitro* kinase assay and histone methylation assay.** For the *in vitro* phosphorylation assay, anti-Flag–NLK immunocomplexes were incubated with GST–SETDB1 (WT, T700A and T976A) in 10 μl of kinase buffer containing 10 mM HEPES (pH 7.4), 1 mM dithiothreitol (DTT), 5 mM $MgCl_2$ and 5 μCi of [γ^{32}P]ATP at 25 °C for 10 min. Samples were resolved by SDS polyacrylamide gel electrophoresis (SDS-PAGE), and phosphorylated proteins were visualized by imaging analyser BAS1500 (Fujifilm, Tokyo, Japan). For the histone methyltransferase assay, we used aliquots of anti-Flag–NLK immunocomplexes and the HMT assay kit (Upstate).

Protein purification. For NLK–PPAR-γ complex purification, HeLa cells stably expressing Flag–NLK were incubated with 50 mM KCl for 30 min, and nuclear extracts were prepared as previously described[37,38]. Then extracts were bound to the GST–PPAR-γ column, and complexes bound to PPAR-γ were eluted with 15 mM reduced glutathione in elution buffer (50 mM Tris-HCl, pH 8.3, 150 mM KCl, 0.5 mM EDTA, 0.5 mM PMSF, 5 mM CHD7, 0.08% NP-40 and 10% glycerol) and loaded onto an anti-Flag M2 resin column (Sigma, St Louis, MO), washed with binding buffer, and eluted by incubation for 60 min with 0.5 ml of the Flag peptide (0.2 mg ml^{-1}) (Sigma) in binding buffer. After elution, proteins were identified by MALDI-TOF mass spectroscopy (Voyager, Applied Biosystems, Foster City, CA). For glycerol density gradient fractionation, they were layered on top of a 4.5 ml linear 100%–40% glycerol gradient in the binding buffer and centrifuged for 16 h at 4 °C at 40,000 r.p.m. in a SW40 rotor (Beckman Coulter, Fullerton, CA).

Pull-down assays. NLK (amino acids 1–443, 124–517), SETDB1 (amino acids 661–1291), PPAR-γ mutants (amino acids 1–138, 139–311, 204–506, 1–506) were expressed as a GST fusion protein in *Escherichia coli* strain HB101. The expression of a protein of the predicted size was then monitored by SDS-PAGE. GST pull-down assays using [^{35}S]-methionine-labelled CHD7, CHD7$^{1\text{-}1107}$, NLK and SETDB1 were performed as previously described[15]. Peptide pull-down assays using GST–CHD7 (amino acids 231–364) were performed as previously described[50]. For histone-binding assays, GST proteins were incubated with semi-purified HeLa histones in 300 mM NaCl, 50 mM Tris-HCl (pH 7.5), 5 mM EDTA (pH 7.9), 0.5% NP40 for 2 h at room temperature. After washing three times in 500 mM NaCl, 50 mM Tris-HCl (pH 7.5), 5 mM EDTA (pH 7.9), 0.5% NP40, samples were separated by SDS-PAGE and western blotting was performed.

Adenoviral constructs and transduction. The adenoviral vector expressing RNAi against murine *NLK*, murine *SETDB1*, and murine *CHD7* were constructed from pSIREN and Adeno-X (Clontech, Palo Alto, CA). The RNAi oligonucleotide sequences are as follows: Control, CTGGACTTCCAGAAGAAATT; *NLK*, GCAGCCGTCATTACAGCAA; *SETDB1*, GGTGATGAGTACTTTGCAA; *CHD7*, GCAATCATCCCTACCTAAT. Adeno-X plasmids were digested with *PacI* and cotransfected into 293T cells using Lipofectamine Plus (Invitrogen, Carlsbad, CA). Virus-containing supernatants were collected at 48 h post-transfection and passed through a 0.45 μm filter.

Note: Supplementary Information is available on the Nature Cell Biology website.

ACKNOWLEDGEMENTS

We thank A. P. Kouzmenko, M. Kim and R. Fujiki for helpful discussions and H. Higuchi and S. Fujiyama for manuscript preparation. And we also thank S. Ishii (RIKEN Tsukuba Institute) for helpful advice and T. Komori (Nagasaki University) for the kind gift of the *Runx2* expression vector and reporter vector. This work was supported, in part, by a Grant-In-Aid for Basic Research Activities for Innovative Biosciences (BRAIN) and Priority Areas from the Ministry of Education, Science, Sports, and Culture of Japan (to S.K.).

Published online at http://www.nature.com/naturecellbiology/
Reprints and permissions information is available online at http://npg.nature.com/reprintsandpermissions

1. Fischle, W., Wang, Y. & Allis, C. D. Histone and chromatin cross-talk. *Curr. Opin. Cell Biol.* **15,** 172–183 (2003).
2. Margueron, R., Trojer, P. & Reinberg, D. The key to development: interpreting the histone code? *Curr. Opin. Genet. Dev.* **15,** 163–176 (2005).
3. Martin, C. & Zhang, Y. The diverse functions of histone lysine methylation. *Nature Rev. Mol. Cell Biol.* **6,** 838–849 (2005).
4. Bannister, A. J. & Kouzarides, T. Reversing histone methylation. *Nature* **436,** 1103–1106 (2005).
5. Metzger, E., Wissmann, M. & Schule, R. Histone demethylation and androgen-dependent transcription. *Curr. Opin. Genet. Dev.* **16,** 513–517 (2006).
6. Wu, R. C., Smith, C. L. & O'Malley, B. W. Transcriptional regulation by steroid receptor coactivator phosphorylation. *Endocr. Rev.* **26,** 393–399 (2005).
7. Dilworth, F. J. & Chambon, P. Nuclear receptors coordinate the activities of chromatin remodeling complexes and coactivators to facilitate initiation of transcription. *Oncogene* **20,** 3047–3054 (2001).
8. Rosenfeld, M. G., Lunyak, V. V. & Glass, C. K. Sensors and signals: a coactivator/corepressor/epigenetic code for integrating signal-dependent programs of transcriptional response. *Genes Dev.* **20,** 1405–1428 (2006).
9. Pascual, G. *et al.* A SUMOylation-dependent pathway mediates transrepression of inflammatory response genes by PPAR-gamma. *Nature* **437,** 759–763 (2005).
10. Evans, R. M., Barish, G. D. & Wang, Y. X. PPARs and the complex journey to obesity. *Nature Med.* **10,** 355–361 (2004).
11. Feige, J. N., Gelman, L., Michalik, L., Desvergne, B. & Wahli, W. From molecular action to physiological outputs: peroxisome proliferator-activated receptors are nuclear receptors at the crossroads of key cellular functions. *Prog. Lipid Res.* **45,** 120–159 (2006).
12. Lehrke, M. & Lazar, M. A. The many faces of PPARgamma. *Cell* **123,** 993–999 (2005).
13. Tontonoz, P., Hu, E., Graves, R. A., Budavari, A. I. & Spiegelman, B. M. mPPAR gamma 2: tissue-specific regulator of an adipocyte enhancer. *Genes Dev.* **8,** 1224–1234 (1994).
14. Hu, E., Kim, J. B., Sarraf, P. & Spiegelman, B. M. Inhibition of adipogenesis through MAP kinase-mediated phosphorylation of PPARgamma. *Science* **274,** 2100–2103 (1996).
15. Suzawa, M. *et al.* Cytokines suppress adipogenesis and PPAR-gamma function through the TAK1/TAB1/NIK cascade. *Nature Cell Biol.* **5,** 224–230 (2003).
16. Chien, K. R. & Karsenty, G. Longevity and lineages: toward the integrative biology of degenerative diseases in heart, muscle, and bone. *Cell* **120,** 533–544 (2005).
17. Harada, S. & Rodan, G. A. Control of osteoblast function and regulation of bone mass. *Nature* **423,** 349–355 (2003).
18. Ralston, S. H. & de Crombrugghe, B. Genetic regulation of bone mass and susceptibility to osteoporosis. *Genes Dev.* **20,** 2492–2506 (2006).
19. Behrens, J. *et al.* Functional interaction of beta-catenin with the transcription factor LEF-1. *Nature* **382,** 638–642 (1996).
20. Ishitani, T. *et al.* The TAK1-NLK mitogen-activated protein kinase cascade functions in the Wnt-5a/Ca(2+) pathway to antagonize Wnt/beta-catenin signaling. *Mol. Cell. Biol.* **23,** 131–139 (2003).
21. Veeman, M. T., Axelrod, J. D. & Moon, R. T. A second canon. Functions and mechanisms of beta-catenin-independent Wnt signaling. *Dev. Cell* **5,** 367–377 (2003).
22. Schultz, D. C., Ayyanathan, K., Negorev, D., Maul, G. G. & Rauscher, F. J. 3rd. SETDB1: a novel KAP-1-associated histone H3, lysine 9-specific methyltransferase that contributes to HP1-mediated silencing of euchromatic genes by KRAB zinc-finger proteins. *Genes Dev.* **16,** 919–932 (2002).
23. Wang, H. *et al.* mAM facilitates conversion by ESET of dimethyl to trimethyl lysine 9 of histone H3 to cause transcriptional repression. *Mol. Cell* **12,** 475–487 (2003).
24. Vissers, L. E. *et al.* Mutations in a new member of the chromodomain gene family cause CHARGE syndrome. *Nature Genet.* **36,** 955–957 (2004).
25. Komatsu, Y. *et al.* Targeted disruption of the Tab1 gene causes embryonic lethality and defects in cardiovascular and lung morphogenesis. *Mech. Dev.* **119,** 239–249 (2002).
26. Ishitani, T. *et al.* The TAK1-NLK-MAPK-related pathway antagonizes signalling between beta-catenin and transcription factor TCF. *Nature* **399,** 798–802 (1999).
27. Almind, K. & Kahn, C. R. Genetic determinants of energy expenditure and insulin resistance in diet-induced obesity in mice. *Diabetes* **53,** 3274–3285 (2004).
28. Mueller, E. *et al.* Terminal differentiation of human breast cancer through PPAR gamma. *Mol. Cell* **1,** 465–470 (1998).
29. Hong, J. H. *et al.* TAZ, a transcriptional modulator of mesenchymal stem cell differentiation. Science **309,** 1074–1078 (2005).
30. Schwartz, A. V. *et al.* Thiazolidinedione use and bone loss in older diabetic adults. *J. Clin. Endocrinol. Metab.* **91,** 3349–3354 (2006).
31. Akune, T. *et al.* PPARgamma insufficiency enhances osteogenesis through osteoblast formation from bone marrow progenitors. *J. Clin. Invest.* **113,** 846–855 (2004).
32. Takada, S. *et al.* Wnt-3a regulates somite and tailbud formation in the mouse embryo. *Genes Dev.* **8,** 174–189 (1994).
33. Glass, D. A. 2nd *et al.* Canonical Wnt signaling in differentiated osteoblasts controls osteoclast differentiation. *Dev. Cell* **8,** 751–764 (2005).
34. Gong, Y. *et al.* LDL receptor-related protein 5 (LRP5) affects bone accrual and eye development. *Cell* **107,** 513–523 (2001).
35. Ross, S. E. *et al.* Inhibition of adipogenesis by Wnt signaling. *Science* **289,** 950–953 (2000).
36. Yamaguchi, T. P., Bradley, A., McMahon, A. P. & Jones, S. A Wnt5a pathway underlies outgrowth of multiple structures in the vertebrate embryo. *Development* **126,** 1211–1223 (1999).
37. Kitagawa, H. *et al.* The chromatin-remodeling complex WINAC targets a nuclear receptor to promoters and is impaired in Williams syndrome. *Cell* **113,** 905–917 (2003).
38. Yanagisawa, J. *et al.* Nuclear receptor function requires a TFTC-type histone acetyl transferase complex. *Mol. Cell* **9,** 553–562 (2002).
39. Brehm, A., Tufteland, K. R., Aasland, R. & Becker, P. B. The many colours of chromodomains. *Bioessays* **26,** 133–140 (2004).
40. Botrugno, O. A. *et al.* Synergy between LRH-1 and beta-catenin induces G1 cyclin-mediated cell proliferation. *Mol. Cell* **15,** 499–509 (2004).
41. Kouzmenko, A. P. *et al.* Wnt/beta-catenin and estrogen signaling converge *in vivo*. *J. Biol. Chem.* **279,** 40255–40258 (2004).
42. Asahina, M., Valenta, T., Silhankova, M., Korinek, V. & Jindra, M. Crosstalk between a nuclear receptor and beta-catenin signaling decides cell fates in the *C. elegans* somatic gonad. *Dev. Cell* **11,** 203–211 (2006).
43. Zhu, P. *et al.* Macrophage/cancer cell interactions mediate hormone resistance by a nuclear receptor derepression pathway. *Cell* **124,** 615–629 (2006).
44. Garcia-Bassets, I. *et al.* Histone methylation-dependent mechanisms impose ligand dependency for gene activation by nuclear receptors. *Cell* **128,** 505–518 (2007).
45. Wang, J. *et al.* Opposing LSD1 complexes function in developmental gene activation and repression programmes. *Nature* **446,** 882–887 (2007).
46. Kurahashi, T., Nomura, T., Kanei-Ishii, C., Shinkai, Y. & Ishii, S. The Wnt-NLK signaling pathway inhibits A-Myb activity by inhibiting the association with coactivator CBP and methylating histone H3. *Mol. Biol. Cell* **16,** 4705–4713 (2005).
47. Kubota, N. *et al.* PPAR gamma mediates high-fat diet-induced adipocyte hypertrophy and insulin resistance. *Mol. Cell* **4,** 597–609 (1999).
48. Ohtake, F. *et al.* Modulation of oestrogen receptor signalling by association with the activated dioxin receptor. *Nature* **423,** 545–550 (2003).
49. Fujiwara, M. *et al.* Isolation and characterization of the distal promoter region of mouse Cbfa1. *Biochim. Biophys. Acta* **1446,** 265–272 (1999).
50. Fujiki, R. *et al.* Ligand-induced transrepression by VDR through association of WSTF with acetylated histones. *EMBO J.* **24,** 3881–3894 (2005).

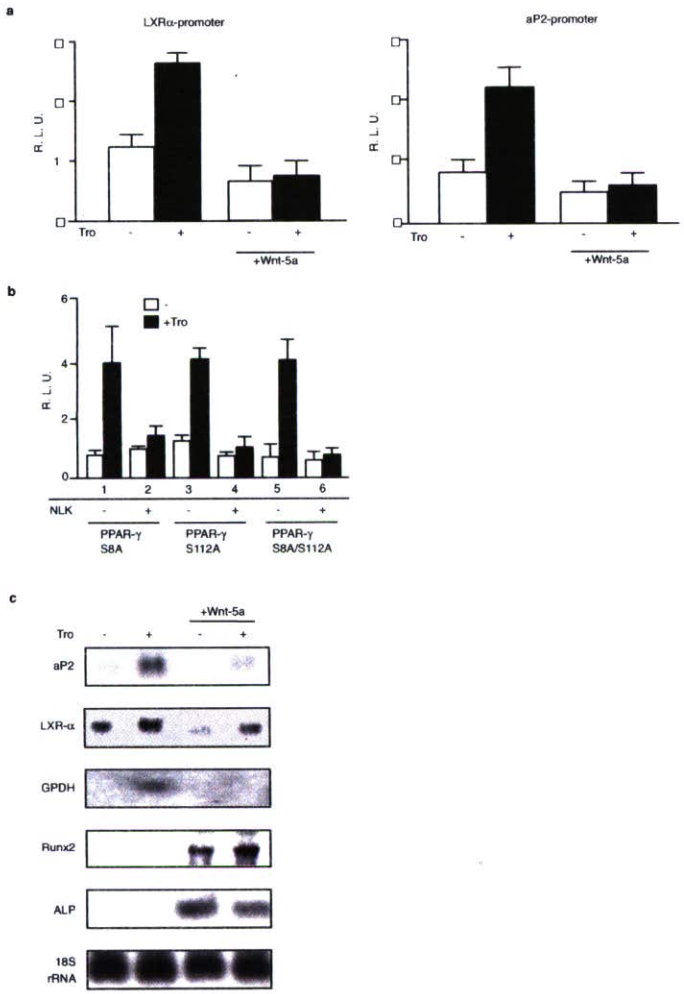

Figure S1. Supplemental data on luciferase reporter assays. (**a**) Luciferase assay in ST2 cells. After transfection with expression vectors of PPAR-γ and each reporter vectors ST2 cells were cultured with or without Wnt-5a for 24hrs and luciferase assay was performed. (**b**) Lusiferase assay in ST2 cells transfected with expression vectors of MAPK phosphorylation mutants of PPAR-γ (S8A, S112A, S8A-S112A), NLK and PPRE-tk-luc vectors. In (**a**) and (**b**), error bars represent the means +/- S. D. of triplicate, independent determinations. (**c**) Northern blot analysis for differentiation markers of adipocytes (aP2, GPDH and LXR-α) and osteoblasts (ALP and Runx2) in ST2 cells incubated with or without Wnt-5a and Tro were performed.

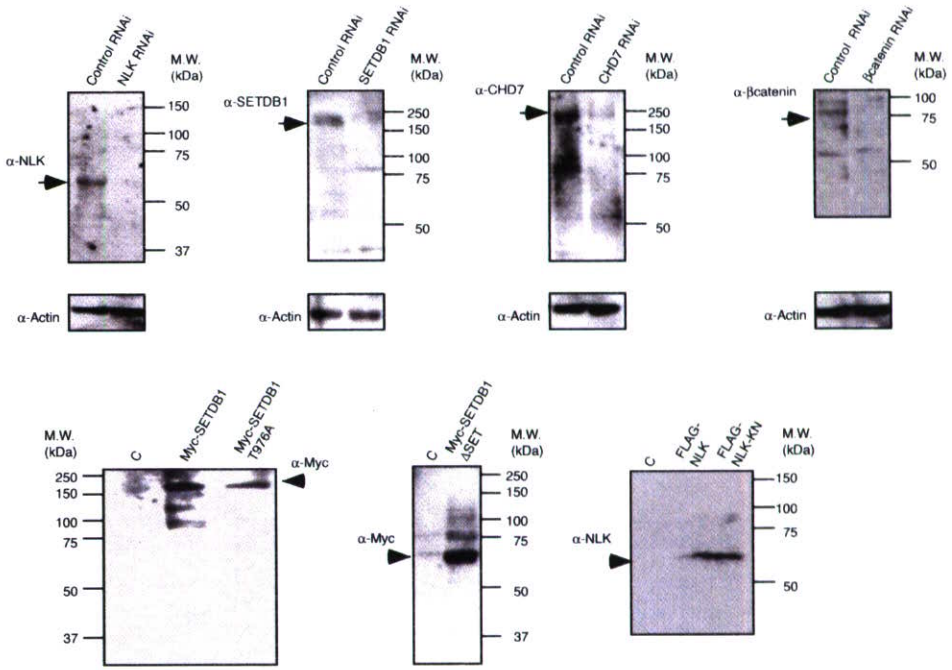

Figure S2. Supplemental data on protein expression. Each nuclear-cell extracts were prepared and then western blotting was performed.

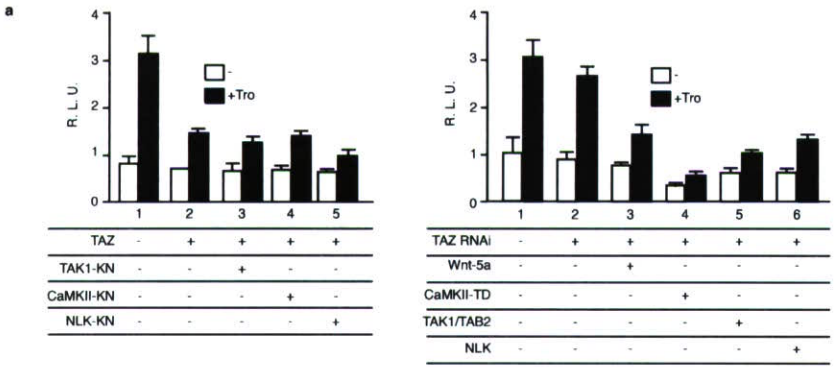

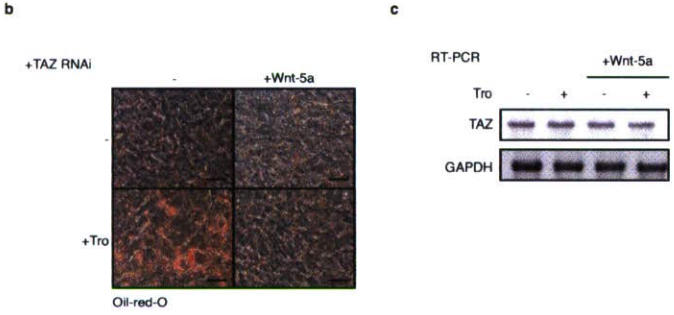

Figure S3. Supplemental data on TAZ function in Wnt-5a signaling. (**a**) Luciferase assay transfected with PPRE-tk-luc vector and indicated vectors were performed. Error bars represent the means +/- S. D. of triplicate, independent determinations. (**b**) TAZ RNAi did not abrogate Wnt-5a induced inhibition of adipogenesis. ST2 cells were transfected with adenovirus expressing mTAZ-specific RNAi and were then transferred to adipocyte differentiation medium. Cells were stained by Oil-red O. Scale bars, 100 μm. (**c**) Expression level of TAZ mRNA was not changed when treated with or without Tro or Wnt-5a in (**b**). RT-PCR was performed.

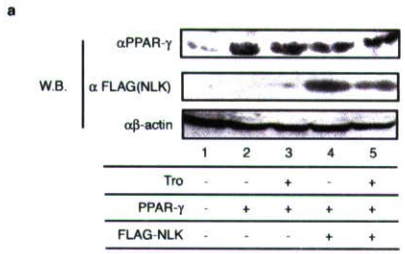

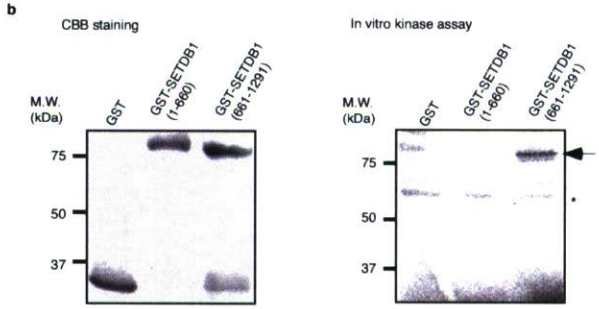

Figure S4. (a) Supplemental data on the degradation of PPAR-γ by NLK. ST2 cells were transfected with NLK expression vector and then lysates were performed for western blotting with antibody against PPAR-γ. **(b)** In vitro kinase assay using GST, GST-SETDB1 (1-660 amino aicds), and GST-SETDB1 (661-1291 amino acids). GST fused proteins were incubated with anti-FLAG-NLK immunocomplexes and [^{32}P]γ-ATP. Arrow head indicates phosphorylated GST-SETDB1 (661-1291 amino acids) and asterisk indicates self-phosphoerylated NLK.

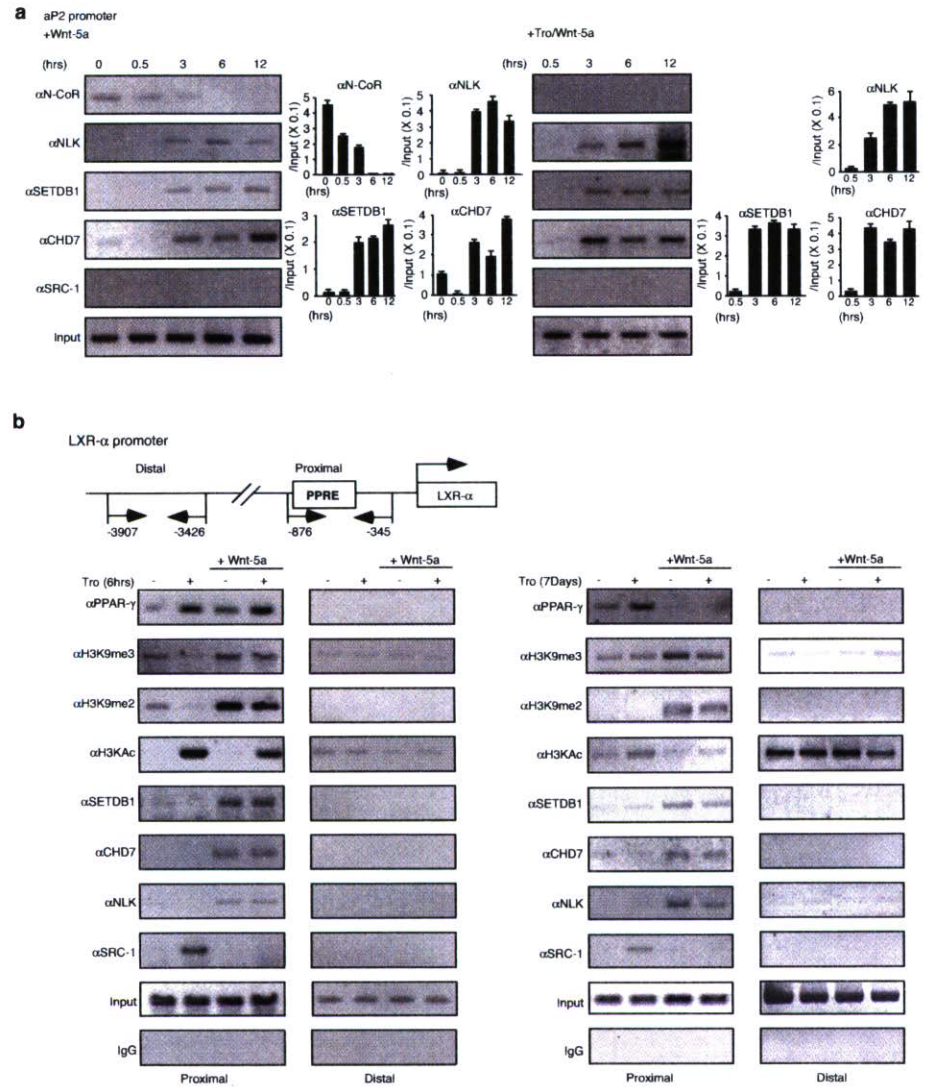

Figure S5. Supplemental data on the ChIP analysis. (**a**) Time-coursed ChIP analysis on aP2 promoter in ST2 cells. After treated with or without Tro or Wnt-5a, each time-coursed ChIP analysis was performed by using indicated antibodies. Recruitment intensity was shown as each graph. Error bars represent the means +/- S. D. of triplicate, independent determinations. (**b**) ChIP analysis on LXR-α promoter in ST2 cells. ST2 cells were treated with/without Tro and Wnt-5a for 6 hrs (left panel) or 7days (right panel). Then ChIP analysis was performed with indicated antibodies on LXR-α promoter region.

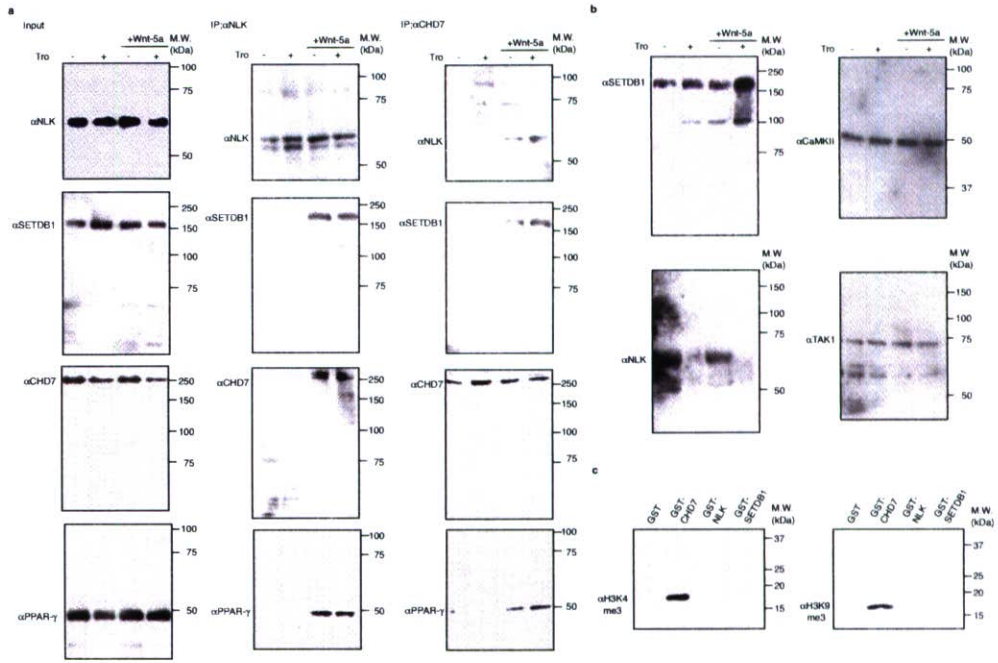

Figure S6. Selected representative full-scan images. Full sized membranes were cut prior to immunoblotting according to prestained MW markers. (**a**) Images correspond to Fig. 4e. (**b**) Images correspond to Fig. 5a left panel. (**c**) Images correspond to Fig. 5g.

Reference

1. Hong, J. H. et al. TAZ, a transcriptional modulator of mesenchymal stem cell differentiation. Science 309, 1074-8 (2005).

Supplementary Information

MATERIALS

The primers used for quantitative RT-PCR were as follows;

aP2; 5'-TGGGAACCTGGAAGCTTGTCTC-3' for forward primer and 5'-GCTGATGATCATGTTGGGCTTG-3' for reverse primer.

ALP; 5'-ACACCTTGACTGTGGTTCTGCTGA-3' for forward primer and 5'-CCTTGTAGCCAGGCCCGTTA-3' for reverse primer.

Runx2; 5'-CATTTGCACTGGGTCACACGTA-3' for forward primer and 5'-GAATCTGGCCATGTTTGTGCTC-3' for reverse primer.

LXR-α; 5'-TGCAGGACCAGCTCCAAGTAGA-3' for forward primer and 5'-GGCTCACCAGCTTCATTAGCATC-3' for reverse primer.

GPDH; 5'-GGGCTGAAGCTAATCTCCGACA-3' for forward primer and 5'-AGGCCGTTCTGCTCACTTTG-3' for reverse primer.

ChIP analysis was performed as described in the text. Used primers for ChIP analysis were 5'-AGTTCAGCACAGAAGTGCTTTCCTAGC-3' (-876 to -850) and 5'-CCCATCTGAGATGGTGTCAAGATCTAC-3' (-372 to -345) for the LXR-α gene promoter region at PPRE, and 5'-CGCCCGGATGCATTCGTAAGGA-3' (-3907 to -3886) and 5'-GGCTGGTTACATGCAGTACCCT-3' (-3447 to -3426) for LXR-α gene distal region.

Reporter vectors of aP2 promoter (-4246 to -6025)-tk-luc or LXR-α promoter (-1 to

-1650)-tk-luc were cloned by PCR and inserted into pGL3-tk-luc. Mouse TAZ1 cDNA was cloned by PCR and inserted into pcDNA3. RNAi sequence of TAZ1 was same as previously described[1]. Primers for RT-PCR were as follows; Fw; 5'-AATCCGTCCTCGGTGCCCCATCCGC-3', Rev; 5'-TTACAGCCAGGTTAGAAAGG-3'.

The EMBO Journal (2007) 26, 764–774 | © 2007 European Molecular Biology Organization | All Rights Reserved 0261-4189/07
www.embojournal.org

THE EMBO JOURNAL

A cell cycle-dependent co-repressor mediates photoreceptor cell-specific nuclear receptor function

Shinichiro Takezawa[1,4], Atsushi Yokoyama[1], Maiko Okada[1], Ryoji Fujiki[1], Aya Iriyama[2], Yasuo Yanagi[2], Hiroaki Ito[1], Ichiro Takada[1], Masahiko Kishimoto[1], Atsushi Miyajima[1], Ken-ichi Takeyama[1], Kazuhiko Umesono[3], Hirochika Kitagawa[1] and Shigeaki Kato[1,4,*]

[1]The Institute of Molecular and Cellular Biosciences, University of Tokyo, Bunkyo-ku, Tokyo, Japan, [2]Department of Ophthalmology, University of Tokyo, School of Medicine, Bunkyo-ku, Tokyo, Japan, [3]Institute for Virus Research, and Graduate School for Biostudies, Kyoto University, Kyoto, Japan and [4]ERATO, Japan Science and Technology Agency, Kawaguchi, Saitama, Japan

Photoreceptor cell-specific nuclear receptor (PNR) (NR2E3) acts as a sequence-specific repressor that controls neuronal differentiation in the developing retina. We identified a novel PNR co-repressor, Ret-CoR, that is expressed in the developing retina and brain. Biochemical purification of Ret-CoR identified a multiprotein complex that included E2F/Myb-associated proteins, histone deacetylases (HDACs) and NCoR/HDAC complex-related components. Ret-CoR appeared to function as a platform protein for the complex, and interacted with PNR via two CoRNR motifs. Purified Ret-CoR complex exhibited HDAC activity, co-repressed PNR transrepression function *in vitro*, and co-repressed PNR function in PNR target gene promoters, presumably in the retinal progenitor cells. Notably, the appearance of Ret-CoR protein was cell-cycle-stage-dependent (from G1 to S). Therefore, Ret-CoR appears to act as a component of an HDAC co-repressor complex that supports PNR repression function in the developing retina, and may represent a co-regulator class that supports transcriptional regulator function via cell-cycle-dependent expression.

The EMBO Journal (2007) **26,** 764–774. doi:10.1038/sj.emboj.7601548; Published online 25 January 2007
Subject Categories: chromatin & transcription
Keywords: cell cycle; co-repressor complex; HDAC; PNR; retina

Introduction

Members of the nuclear receptor (NR) gene superfamily serve as sequence-specific regulators in the promoters of their cognate target genes (Mangelsdorf *et al*, 1995). Reflecting the spatiotemporal expression patterns of NRs in animals, a wide variety of biological events are under the control of NR-mediated transcriptional regulation (McKenna and O'Malley, 2002; Rosenfeld *et al*, 2006). Structurally, NR proteins can be divided into five domains, A–E. The highly conserved C domain acts as a DNA-binding domain (DBD), which has two Zn-finger motifs that recognize and stably bind to specific target DNA sequences. The moderately conserved ligand-binding domain (LBD) is mapped to the C-terminal E domain. The N-terminal A/B domain exhibits poor homology among NRs but is responsible for ligand-induced transactivation together with the LBD regions in NRs such as nuclear hormone/vitamin receptors. Unlike hormone/vitamin receptors, several NRs are believed not to require ligand binding, and are therefore classified as orphan receptors that function as ligand-independent regulators (Mangelsdorf *et al*, 1995).

Ligand-dependent and -independent transcriptional control by NRs requires histone modification and chromatin remodeling (Belandia and Parker, 2003; Kitagawa *et al*, 2003). Histone modification coupled with transcriptional control by NRs depends on the input of two types of co-regulators with opposing functions. It appears that most co-regulators exist as multiprotein complexes (McKenna and O'Malley, 2002; Perissi and Rosenfeld, 2005). It is thought that three distinct classes of co-activators support NR transactivation, with two of these classes, CBP/p160 and GCN5/TRPAP complexes (Onate *et al*, 1995; Kamei *et al*, 1996; Yanagisawa *et al*, 2002), containing histone acetyltransferase (HAT) enzymes. The other class, DRIP/TRAP complex, is a non-HAT co-activator complex (Fondell *et al*, 1996; Rachez *et al*, 1999). The co-repressor type complexes contain histone deacetylase (HDAC) enzymes, which along with NCoR/SMRT physically interact with NRs via CoRNR motifs, and are thought to be functionally indispensable subunits in NR co-repression complexes (Heinzel *et al*, 1997; Nagy *et al*, 1997). The other histone-modifying enzymes are also likely to co-regulate the NR function (Metzger *et al*, 2005). Although histone modification owing to HAT/HDAC activity in NR co-regulator complexes may in cooperation with chromatin-remodeling complexes explain at least in part the mechanism of NR-mediated transcriptional control via chromatin remodeling (Narlikar *et al*, 2002; Belandia and Parker, 2003; Kitagawa *et al*, 2003), the molecular link between NR-mediated gene regulation and cell cycle control remains elusive.

The photoreceptor-specific orphan receptor PNR (NR2E3) is a pivotal regulator in the developing retina, as it determines cone photoreceptor phenotype (Haider *et al*, 2001; Milam *et al*, 2002; Yanagi *et al*, 2002). Its significance in neuronal differentiation has been established by a number of studies based on spontaneous genetic mutations of the PNR gene in human enhanced S-cone syndrome (ESCS) patients and in rd7/rd7 mice, which suffer retinal degeneration and lack color perception due to imbalanced ratio between S- and M-cone cell numbers (Akhmedov *et al*, 2000; Gerber *et al*, 2000; Haider *et al*, 2000). PNR appears to attenuate cell proliferation of S-cone cells from retinal progenitor cells, but is unlikely to control of differentiation of S into M-cone cells.

Given that the well-known NR co-repressor NCoR/SMRT was not potent to co-repress PNR (see Figure 1F), we identified a novel PNR co-repressor, designated as Ret-CoR. By a biochemical approach, Ret-CoR was shown to form an HDAC complex to co-repress PNR. Most notably, appearance of Ret-CoR protein was dependent on cell cycle. Thus, Ret-CoR may represent a novel class of co-regulators that support transcriptional function of sequence-specific regulators via cell cycle-dependent expression.

*Corresponding author. Institute of Molecular and Cellular Biosciences, University of Tokyo, Yayoi, Bunkyo-ku, Tokyo 113-0032, Japan. Tel.: +81 3 5841 8478; Fax: +81 3 5841 8477; E-mail: uskato@mail.ecc.u-tokyo.ac.jp

Received: 9 November 2006; accepted: 15 December 2006; published online: 25 January 2007

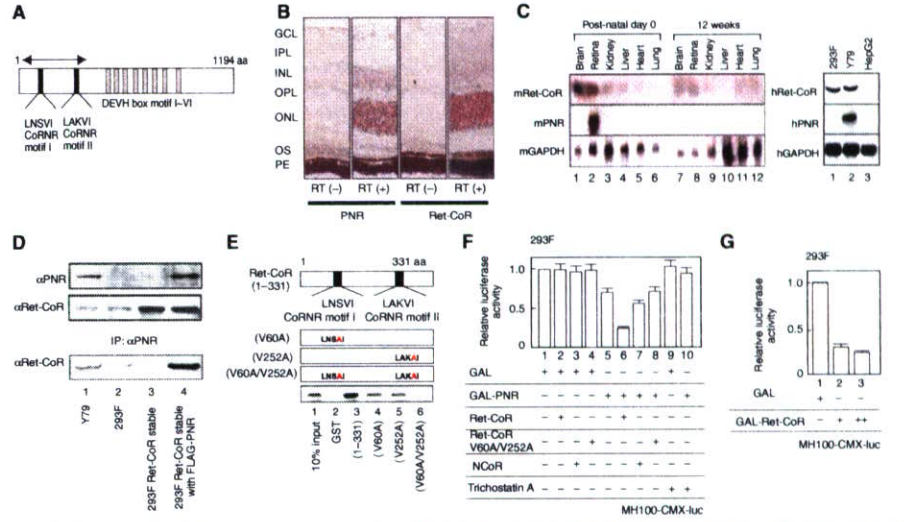

Figure 1 Identification of Ret-CoR as a novel co-repressor of an orphan nuclear receptor PNR. (**A**) Schematic diagram of Ret-CoR protein. The two CoRNR motifs, DEVH box motifs and the region corresponding to the isolated cDNA clone (arrows) by yeast two-hybrid screening are illustrated. (**B**) Expression of Ret-CoR transcripts in the retina. *In situ* RT–PCR of adult mouse retinal sections performed with [RT(+)] or without [RT(−)] reverse transcriptase (RT). PNR (left) and Ret-CoR (right) transcripts as detected by *in situ* RT–PCR are shown. GCL, ganglion cell layer; IPL, inner plexiform layer; INL, inner nuclear layer; OPL, outer nuclear layer; OS, outer segment; PE, pigment epithelium. (**C**) Expression of Ret-CoR and PNR transcripts in mouse tissue (left panel) and human culture cells (right panel) as determined by Northern blotting. (**D**) Interaction between PNR and Ret-CoR in each cell line. Whole cell extracts from Y79 cells, 293F cells, and untransfected/PNR-transfected 293F Ret-CoR stable cells were subjected to immunoprecipitation (IP) with anti-PNR antibody. Each immunoprecipitant was then analyzed by Western blot (IB) with anti-PNR or anti-Ret-CoR antibody. (**E**) The CoRNR motif of Ret-CoR mediates interaction with PNR. *In vitro*-translated PNR proteins were applied for a GST pull-down assay. (**F**) Ret-CoR mediates the co-repressive function of PNR. Luciferase assays were performed in 293F cells transfected with a GAL4-DBD-binding site × 4 containing luciferase reporter plasmid (MH100-CMX-luc) (400 ng), GAL-fused expression vectors (200 ng), Ret-CoR expression vectors (100 ng), NCoR expression vectors (100 ng) and 10^{-9} M Trichostatin A. (**G**) Ret-CoR has a transrepressive activity itself. Luciferase assays were performed as illustrated in (F) using GAL-fused Ret-CoR expression vectors (200 ng (+) or 500 ng (++)).

Results

Identification of Ret-CoR as a novel PNR co-repressor

We used the yeast two-hybrid system to screen a human brain cDNA library for putative co-repressors that supported the constitutive transrepression function of PNR. We identified a specific PNR-interacting clone that encoded the N-terminal region of the KIAA0890 protein (Nagase *et al*, 1998). Full-length KIAA0890 sequence encoded a 1194-amino acid-protein that contained a DEVH box motif (ATPase/helicase domain) and two CoRNR motifs (Figure 1A) that are thought to function as a physical interface for nuclear receptors and are found in co-repressors such as NCoR and SMRT (Hu and Lazar, 1999; McKenna and O'Malley, 2002). A mouse ortholog was identified from the NCBI database that showed 98% amino-acid sequence identity to human homologue. *In-situ* RT–PCR performed on slices of mouse retina revealed specific signals of this clone located at specific layers. Like expression pattern of the PNR transcript (Kobayashi *et al*, 1999), the transcript of KIAA0890 appeared to express abundantly in the outer nuclear layer (ONL) and to some extents in inner nuclear layer (INC) of the mouse retina (Figure 1B). whereas significant KIAA0890 mRNA expression was detected in mouse retina and brain tissues on postnatal day 0, levels were significantly decreased in 12-week-old mice, as determined by Northern-blot analysis (Figure 1C). The KIAA0890 gene expressed in the Y79 retinoblastoma cell line, as well as in the human embryonic renal cell line 293F, but PNR transcript was detected only in Y79 (Figure 1C, right panel). Endogenous Ret-CoR protein expression was detectable in Y79 and 293F (Figure 1C), in which nuclear localization of

Ret-CoR protein was observed (data not shown). From the expression pattern, the clone was designated as retina co-repressor (Ret-CoR) hereafter.

To investigate for interactions between PNR and Ret-CoR, we performed co-immunoprecipitation experiments on endogenous PNR and Ret-CoR proteins. Association between the proteins was observed in Y79 cells (Figure 1D), and by *in vitro* GST pull-down assay (data not shown). To map the interacting domain in Ret-CoR, *in vitro*-translated PNR and mutant Ret-CoR GST-fusion proteins were assayed. As expected from previous reports (Hu and Lazar, 1999), disruption of either CoRNR motif (V60A or V252A) in Ret-CoR significantly reduced the interaction with PNR (Figure 1E), which suggested that Ret-CoR interacts with PNR via the two CoRNR motifs.

We then tested the coregulatory function of Ret-CoR by generating a chimeric protein of PNR fused to the yeast GAL4 DNA-binding domain (DBD). A transrepressive activity was detected using the PNR-fusion protein by a transient expression assay in 293F cells (Figure 1F) and Y79 cells (data not shown). As an HDAC inhibitor trichostatin A (TSA) abrogated the transrepression by PNR (see lane 13 in Figure 1F), the HDAC activity was presumed to be required for the PNR-mediated transrepression. Ret-CoR clearly co-repressed PNR transrepression function, whereas NCoR was not so potent in 293F cells (Figure 1F) and the other cell lines (data not shown). Expectedly, TLX (NR2E1), an NR highly homologous to PNR, was also transrepressed by Ret-CoR (data not shown). Ret-CoR on its own exhibited transrepressive activity when fused with GAL4-DBD (Figure 1G). In contrast, this potentiation of transrepression was abrogated (Figure 1F) by point mutations in the Ret-CoR CoRNR motifs (see Figure 1E for the V60A/V252A mutant). Thus, our results indicated that Ret-CoR appears to serve as a co-repressor for PNR.

Ret-CoR forms an HDAC complex

To explore the molecular basis of Ret-CoR co-repressor function, we biochemically purified (Yanagisawa *et al*, 2002; Kitagawa *et al*, 2003) a Ret-CoR-containing complex. We generated stable 293F cell transformants (Ret-CoR-293F) that expressed human Ret-CoR tagged with FLAG and His epitopes at the N- and C-termini, respectively (Figure 2A). Nuclear extracts were then subjected to sequential affinity column purification using an anti-FLAG M2 affinity resin column and then a Protino Ni-affinity column. After concentrating the complexes using glycerol density gradients (Figure 2C), tagged Ret-CoR was detected in fractions that contained a complex with a molecular weight of about 1 MDa (Figure 2C). As shown in Figure 2B, middle panel, Ret-CoR appeared to form a multiprotein complex with 11 polypeptides, which were then identified by a mass spectrometry. The two background proteins appeared Hsc70 and β-actin. The complex formation and subunit identification by MALDI-TOF/MS was further confirmed by immunoprecipitation of the purified complex by an RbAp46-specific antibody (Figure 2B, right panel). Identities of these components in the glycerol density gradient functions could be further confirmed by Western blotting (see Figure 2C). The same Ret-CoR complex components were detected when the endogenous complex was immunoprecipitated of either tagged PNR or Ret-CoR from parent 293F cells by a FLAG antibody (Figure 2D). Similarly, association of endogenous PNR with endogenous complex components in Y79 could be detected by immunoprecipitation with endogenous PNR in Y79 (see Figure 3C).

The Ret-CoR complex components could be grouped into three classes based on putative function: transcription factor E2F-associated co-repressors (Sin3A, p107, HDAC1/2, RbAp48 and RbAp46 (Luo *et al*, 1998)); transcription factor Myb-associated co-repressors (NCoR (Li and McDonnell, 2002), Mybbp1A (Tavner *et al*, 1998; Fan *et al*, 2004) and CDK9 (De Falco *et al*, 2000)); and NCoR/SMRT-associated proteins (HDAC3 (Guenther *et al*, 2000)). Although TBL3 (Weinstat-Saslow *et al*, 1993) and TBL1 (Perissi *et al*, 2004) appear to share similar motif organization, the function of TBL3 has not yet been reported. Using Far Western blotting, we found that PNR interacted with Ret-CoR and CDK9, and that Ret-CoR associated with p107 and TBL3 through its N-terminal domain and with p107 and CDK9 through its C-terminal domain (Figure 2E). These interactions were further confirmed by GST-pull-down assays (Figure 2F). From these findings, we presume that Ret-CoR served as a platform protein capable of promoting assembly of various components into a Ret-CoR complex (as illustrated in Figure 7).

Appearance of the Ret-CoR protein is cell cycle-dependent

Identification of cell-cycle transcription factor-related components related to E2F (Ohtani *et al*, 1995) and Myb (Oh and Reddy, 1999) in the Ret-CoR complex led us to consider a putative role for Ret-CoR in the cell cycle. Expression of Ret-CoR through the cell cycle was investigated by Western blotting using Y79 cells synchronized by thymidine at G1/S stage and demecolcine at G2/M phase (Figure 3A). We found that like endogenous cyclin E, a marker that accumulated mostly during the G1/S transition, appearance of endogenous Ret-CoR protein was dependent on the specific cell-cycle stage from the G1 phase to the S phase (Figure 3B, left panel) when the cells were synchronized by thymidine at G1/S phase (Figure 3A, upper panel). Likewise, when the Y79 cells were synchronized by demecolcine at G2/M phase, Ret-CoR protein appearance was also cell cycle-dependent (Figure 3B, right panel). From these drug studies, the highest Ret-CoR expression (see lower panel in Figure 3B for protein levels of Ret-CoR versus Sin3A) appeared around at G1–S transition (Figure 3A, right panel). A synchronous Y79 cells also expressed Ret-CoR protein, but at low levels (Figure 3B). In the contrast, expression levels of other endogenous Ret-CoR complex components (e.g. Sin3A) and PNR proteins looked unchanged (Figure 3B). As Ret-CoR mRNA levels remained constant during the cell cycle (data not shown), the cell cycle-dependent appearance of Ret-CoR protein appears to be under post-transcriptional control, such as through protein turnover and/or translation rate. In fact, Ret-CoR protein appeared susceptible to ubiquitination for rapid degradation (Figure 3C). Consistent with the Ret-CoR protein appearance during cell cycle, association of endogenous PNR with endogenous Ret-CoR complex components was also dependent on cell cycle and most evident 4 h after G1/S arrest by thymidine (Figure 3D). These findings raised the possibility that the Ret-CoR co-repressor functions as a cell cycle-dependent repressor as well as supporting PNR transrepressive activity. This idea was further supported by the

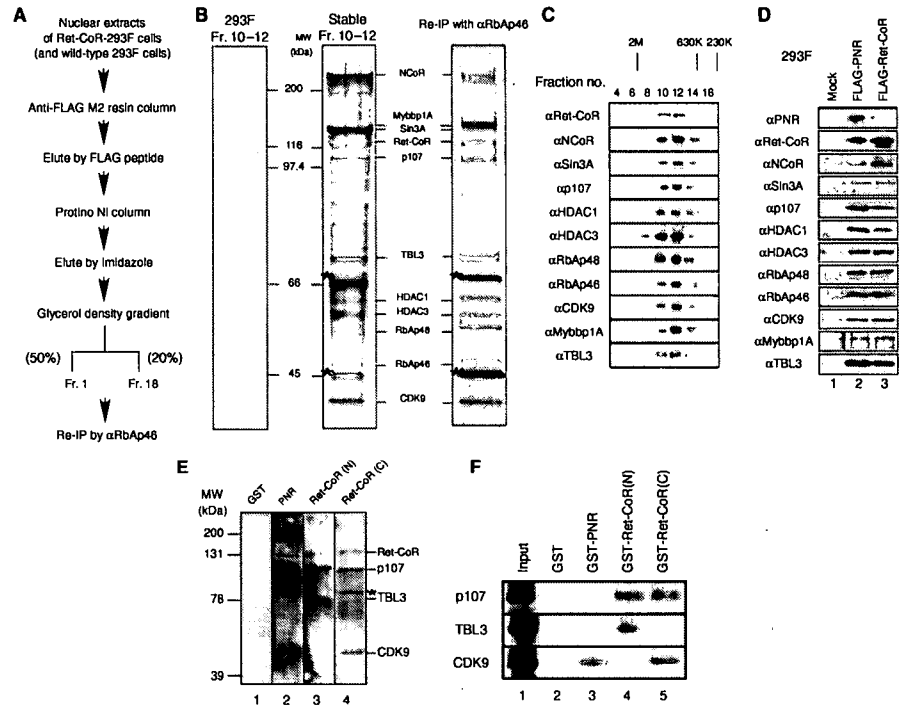

Figure 2 Identification of a novel protein complex containing Ret-CoR. **(A)** Schematic diagram of the purification for Ret-CoR-containing complex. **(B)** Mass spectrometric analysis of the purified Ret-CoR complex components. MALDI-TOF/MS analysis of the complex subunits is shown on the middle. Asterisks indicate background proteins. Silver stain of the indicated fractions of glycerol density gradient were shown at middle panel. Right panel displayed the immunoprecipitant of the purified Ret-CoR complex (middle panel) by anti-RbAp46 antibody (Pre-IP experiment). Left panel displayed immunoprecipitant of Mock cells (wild type 293F cells) precipitated by anti-FLAG M2 resin followed by the same procedure as performed with Ret-CoR complex purification. **(C)** Fractions separated by glycerol density gradient were assayed by Western blot using the indicated antibodies. **(D)** Endogenous components of Ret-CoR complex interact with tagged PNR and Ret-CoR in 293F cells. Immunoprecipitants of tagged PNR and Ret-CoR by a FLAG antibody were applied for Western blotting. **(E)** Far Western blotting of Ret-CoR complexes. Labeled probes were used, as indicated at the top of the panel. The detected bands corresponded to the proteins indicated on the right side. Asterisk indicates a background peptide. **(F)** The Ret-CoR complex components p107, TBL3 and CDK9 directly interact with PNR and Ret-CoR. *In vitro*-translated p107, TBL3 and CDK9 proteins were captured by GST-PNR, Ret-CoR N-terminal and Ret-CoR C-terminal proteins in a GST-pull down assay.

findings that co-transrepression of PNR by Ret-CoR was dependent on cell cycle stage. The PNR-mediated transcription activity was fluctuated during cell cycle and was lowered at the G1/S phase (Figure 3E), when Ret-CoR expression was high. However, by knocking down of Ret-CoR by RNAi (Supplementary Figure 1A) and an HDAC inhibitor Trichostatin A (TSA) treatment, such potent transrepressive activity of PNR at G1–S stages was abrogated (Figure 3E). Likewise, knockdown of combination of CDK9/TBL3, but not single component (only the results of several major components are displayed), resulted in clear impairment of the transrepressive PNR function even when Ret-CoR protein level was presumed high at G1–S stages through synchronization by demecolcine (Figure 3E). These findings supported again the idea that Ret-CoR serves as a co-repressor through forming an HDAC complex.

A purified Ret-CoR complex co-represses the transrepression function of PNR in vitro

To address the co-regulator function of the Ret-CoR complex on PNR, the purified Ret-CoR complex was applied to an *in vitro* transcription assay with a GAL4-DBD-fused PNR LBD chimeric protein (GAL-PNR) and a DNA template chromatinized using purified HeLa histone octamers (Kitagawa *et al*, 2003; Fujiki *et al*, 2005). A basal transcriptional activity was observed from the reporter promoter upon the binding of GAL4-DBD (GAL) alone. However, in the presence of GAL-PNR LBD, the basal activity was drastically reduced (Figure 4A, lane 2), and the addition of the purified Ret-CoR complex potently co-repressed this PNR repressor function (Figure 4A, lane 4). Reflecting the putative role of HDACs in the Ret-CoR complex in co-repression of PNR transrepression function, TSA potently attenuated the

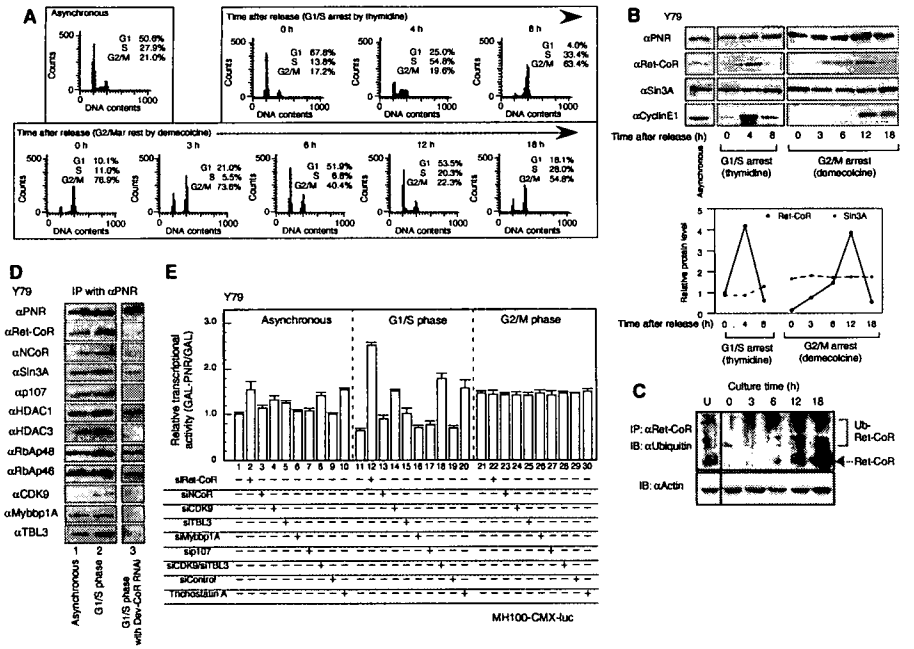

Figure 3 Funcntion of Ret-CoR containing complex is regulated by cell cycle-dependent expression of Ret-CoR. **(A)** FACS analysis of synchronized Y79 cells. Y79 cells were arrested at G1/S phase with thymidine or at G2/M phase with demecolcine. DNA contents of the cells and % populations in each synchronized culture were analyzed by FACS analysis at an indicated time after drug release. **(B)** Expression profiles of PNR and Ret-CoR through the cell cycle. Western blots shows the protein levels indicated in the panel (upper panel). Cyclin E1 was used as a G1/S transition maker. The level in the each step was quantified, normalized in asynchronous cells (lower panel; open circle, Ret-CoR; closed circle, Sin3A). **(C)** Cell cycle-dependent ubiquitination of endogenous Ret-CoR protein. Endogenous Ret-CoR was ubiquitinated in unsynchronized Y79 cells (U) and synchronized Y79 cells treated with MG132 for 3 h, and samples were taken at the indicated times after drug release. Whole cell extracts were immnoprecipitated using anti-Ret-CoR antibody and subjected to Western blotting with antibodies against indicated proteins. **(D)** Ret-CoR is required for the cell cycle-dependent interaction between endogenous Ret-CoR complex components and endogenous PNR in Y79 cells. Proteins were extracted from Y79 cells 4 h after releasing from thymidine treatment. **(E)** Cell cycle-dependent transcriptional repressive function of the Ret-CoR containing complex in Y79 cells. Luciferase assays were performed in asynchronized/synchronized Y79 cells. Relative transcriptional activity means the ratio of the GAL-PNR activity versus activity of GAL alone (GAL-PNR/GAL).

co-repressor function of the purified Ret-CoR complex (Figure 4A, lane 5). Indeed, an HDAC activity was found in the Ret-CoR immunoprecipitant (Figure 4B). When each of the complex components except Ret-CoR was knocked down by RNAi (Supplementary Figure 1A), the Ret-CoR-associated HDAC activity was not altered (Figure 4B). However, knockdown of two components (CDK9 + TBL3) caused a significant reduction in the HDAC activity like the single Ret-CoR RNAi, in accordance with the findings of co-repression of the PNR transrepressive function by the Ret-CoR complex components (Figure 3E). Thus, our findings suggested that the Ret-CoR forms an HDAC complex as a core component to co-repress PNR function.

Ret-CoR co-represses PNR function at the PNR target gene promoter cyclin D1, but not at the TBX2 promoter in Y79 cells

As shown previously in transgenic mice, proliferation in the developing retina requires cyclin D1 (Sicinski *et al*, 1995). Therefore, we reasoned that the expression of this gene, as well as that of the predicted PNR target gene TBX2 (Qian *et al*, 2005), may be under the control of both PNR and Ret-CoR. To test this hypothesis, we first measured the mRNA expression levels of cyclin D1 and TBX2 in Y79 cells by a semi-quantitative RT–PCR. Although no clear expression of cyclin D1 and TBX2 was detected in Y79 cells untransfected and transfected with a control siRNA, after knockdown of PNR expression by RNAi (Supplementary Figure 1A), significant induction of the endogenous Cyclin D1 and TBX2 genes was observed (Figure 5A, lane 2). Ret-CoR RNAi also effectively induced the Cyclin D1 gene, presumably through release of PNR transrepression, but TBX2 gene expression remained repressed (Figure 5A, lane 3). As it is believed that cyclin D1 gene expresses in proliferating retina neurons, whereas TBX2 expresses in differentiated retina (Sowden *et al*, 2001), Ret-CoR was presumed to function in developing retina.

We then directly tested the co-repressor function of Ret-CoR for PNR on PNR target gene promoters (Figure 5B) using

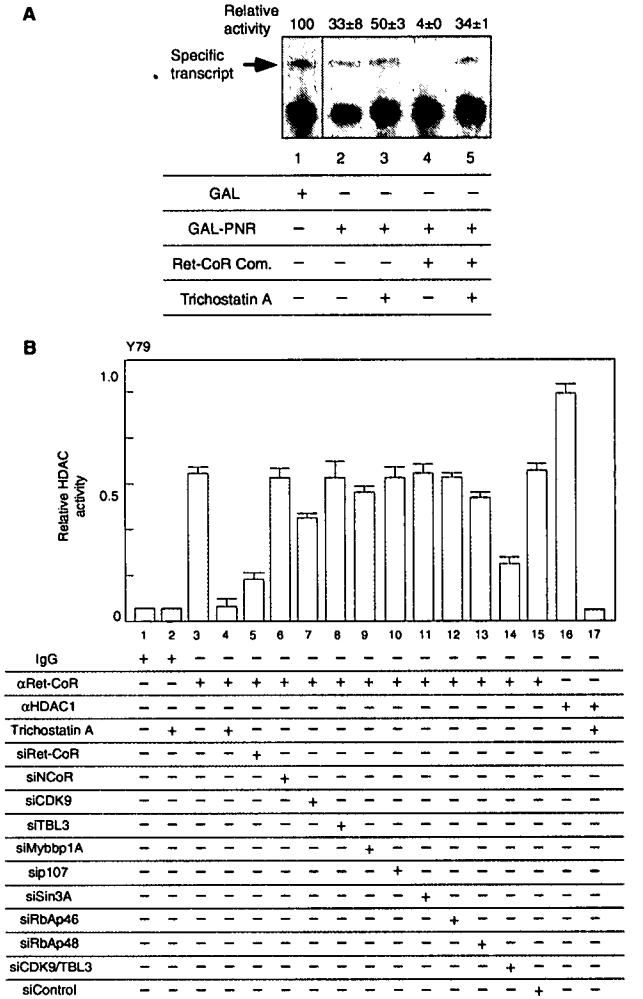

Figure 4 Characterization of the transcriptional repressive function of Ret-CoR containing complex. **(A)** Transrepressional ability of PNR and Ret-CoR were measured with the chromatinized histone octamers and the purified Ret-CoR complex (Figure 2B) by *in vitro* transcription assay. Each assay was performed with or without 500 nM Trichostatin A. **(B)** HDAC activity of a Ret-CoR immnoprecipitants from Y79. Asynchronized whole cell extracts were prepared and immunoprecipitated with either rabbit IgG antibody, anti-Ret-CoR antibody or anti-HDAC1 antibody. Immunoprecipitants were applied on an HDAC assay with or without 10^{-9} M Trichostatin A.

a luciferase reporter and ChIP assays in Y79 cells. The cyclin D1 gene appeared to harbor no putative, or related, PNR-binding sites in its promoter. However, together with a ChIP analysis (Figure 5C and D), functional analysis of promoter deletion mutants (Figure 5E) mapped a putative PNR target region similarly acting in the promoters (L-CycD1-luc and S-CycD1-luc) (see Figure 5B, upper panel). For the TBX2 promoter, recruitment of PNR, but not Ret-CoR, was observed (Figure 5C), which reflected the results of the repressor function experiments (Supplementary Figure 1C). Although PNR among NRs is closely related to TLX that is recently reported as a critical factor for development of neurons including retina (Zhang *et al*, 2006), TLX recruitment was not detected in the PNR target gene promoters (Figure 5C). Conversely, in a TLX target promoter (PTEN) (Zhang *et al*, 2006), neither PNR nor Ret-CoR was recruited (Figure 5C).

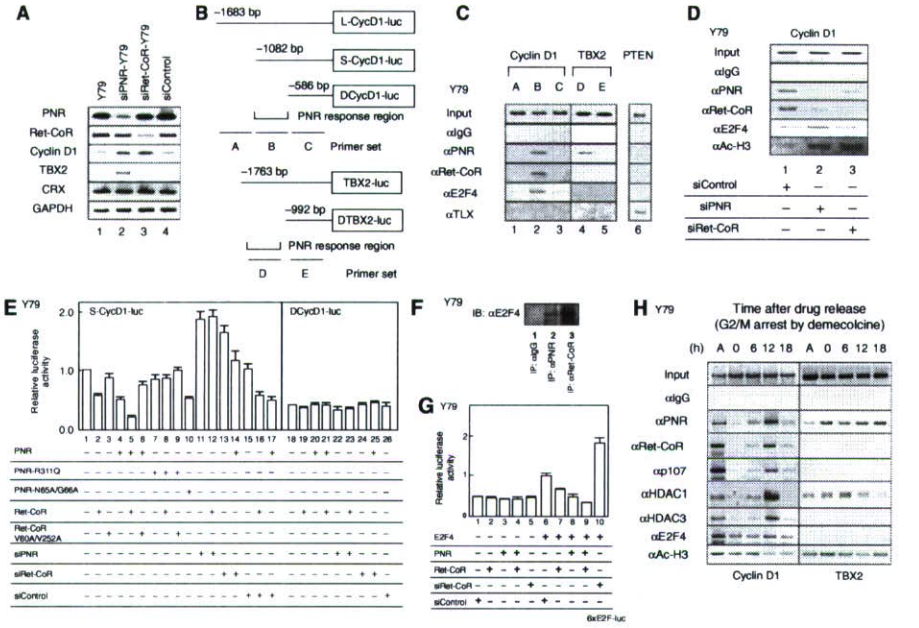

Figure 5 Promoter-specific function of the Ret-CoR containing complex. (**A**) The expression levels of the indicated genes were measured by RT–PCR with extracted total RNA from Y79, transfected with siPNR-Y79, siRet-CoR-Y79 or siControl. (**B**) Schematic diagrams of cyclin D1 promoter and TBX2 promoter with a putative PNR-binding element site. (**C**) ChIP assay was performed to endogenous Cyclin D1 promoter, TBX2 promoter and PTEN promoter with anti-IgG antibody, anti-PNR antibody, anti-Ret-CoR, anti-E2F4 and anti-TLX antibody. (**D**) ChIP assay was performed to Cyclin D1 promoter PNR responsive region (Cyclin D1-B) with anti-IgG antibody, anti-PNR antibody, anti-Ret-CoR antibody and anti-acetyl-Histone H3 treated with transfected siPNR, siRet-CoR or siControl. (**E**) Suppressive effects of PNR and Ret-CoR on Cyclin D1 promoter function. The functions of PNR-CyclinD1-luc (−1082 to 53 bp) or ΔCyclinD1 (−586 to 53 bp) luc promoters in a luciferase assay. (**F**) Co-immunoprecipitation of endogenous E2F4 with endogenous PNR and Ret-CoR. The immunocomplex was precipitated in Y79 cells with anti-PNR or Ret-CoR antibody and Western-blotted with anti-E2F4 antibody. (**G**) Ret-CoR co-represses transcriptional activity of E2F4 on the 6 × E2F response element-containing reporter. Luciferase assays were performed in Y79 cells transfected with 6 × E2F-luc reporter plasmids (400 ng), E2F4 expression vectors (200 ng), Ret-CoR expression vectors (100 ng) and double-stranded siRet-CoR or siControl (20 μM). (**H**) Cell cycle-dependent recruitment of Ret-CoR complex components to Cyclin D1 and TBX2 promoters. ChIP analysis was performed and synchronized Y79 cells at M phase and tested at an indicated time after drug release. Efficiency of synchronization of Y79 cells was determined by FACS as shown in Figure 3A.

A PNR mutant that lacked DNA-binding ability (PNR-N65A/G66A) still potently suppressed Cyclin D1 promoter function (Figure 5E). Notably, the repressive effect of PNR was attenuated by a PNR point mutation (R311Q) found in ESCS patients (Gerber *et al*, 2000; Haider *et al*, 2000), and by mutations in the CoRNR motif (V60A/V252A) of Ret-CoR (Figure 5E). No clear DNA binding of PNR was found in the Cyclin D1 gene promoter region by EMSA (data not shown). To explore further the molecular basis of the transrepressive function of PNR/Ret-CoR in the cyclin D1 gene promoter, we examined an idea if PNR/Ret-CoR associates with E2F family members, as the mapped PNR response element compromises DNA-binding sites for E2F family transcriptional regulators. This idea was further supported by the findings that the isolated Ret-CoR complex contains potential binding components for E2Fs (see Figure 2B). By co-immunoprecipitation, association of endogenous PNR and Ret-CoR proteins with endogenous E2F4 was detected (Figure 5F). Co-repression of E2F4 transcriptional activity by Ret-CoR/PNR was seen in the Cyclin D promoter (L-CycD1-luc) (data not shown) and in the synthetic E2F-binding sites (Figure 5G). Consistent with these findings, recruitment of E2F4 to the promoter Cyclin D, was detectable (Figures 5C, D and H). Moreover, cell cycle-dependent recruitment of PNR and Ret-CoR complex components to regulatory regions in the Cyclin D1 gene promoter was detected by ChIP analysis (Figure 5H). However, for the TBX2 gene promoter, recruitment of PNR, but not Ret-CoR, was observed (Figure 5H). Thus, taken together, our findings suggested that the transrepressive function of PNR in the developing retina requires the co-repressor function of Ret-CoR, presumably as an HDAC complex, with cell cycle-dependent appearance.

Cyclin D1 and TBX2 gene expression is under negative control by PNR in the developing retina

Finally, to address the physiological significance of the observed findings *in vitro*, we measured the expression of PNR and Ret-CoR in the developing retina. Although high PNR and

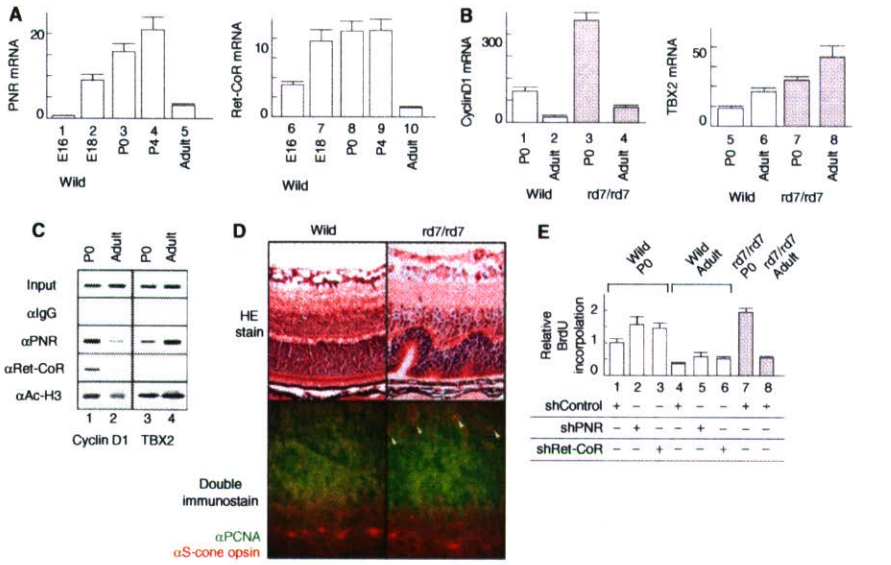

Figure 6 Expression profiles of PNR, Ret-CoR and their target genes during retinal development. (**A**) Transcript levels of the mouse retina at embryonic day 16 to postnatal day 4 and adult phase were quantified by real-time PCR. (**B**) Increased expression of Cyclin D1 and TBX2 as putative PNR/Ret-CoR complex target genes in the retina of wild mice or rd7/rd7 mice quantified by real-time PCR. (**C**) Cyclin D1 and TBX2 promoter occupancy of PNR and Ret-CoR in the mice retina was showed by *in vivo* ChIP assay. (**D**) Hyperproliferation of the retinal progenitor cells. The retina of the wild mice and rd7/rd7 mice at postnatal day 5 were stained with hematoxylin and eosin (upper panel). Rossett formation in the rd7/rd7 mice suggests hyperproliferated S-cone cells from retinal progenitor cells. Sections of developing retinas of wild-type and rd7/rd7 mice at P0 were double-immunostained with as 'green' for PCNA, a marker for dividing retinal progenitor cells and as 'red' for S-cone opsin (lower panel). (**E**) Dissociated retina of the wild mice and rd7/rd7 mice at postnatal day 0- and 12-week old were cultured and incorporated BrdU. Retro virus of control-shRNA (shControl), shPNR or shRet-CoR was infected, respectively.

Ret-CoR expression levels were observed in developing retinas from wild-type mice from stages E18 to P4, only low levels were observed in the mature retina of adult mice (Figure 6A). Further suggestive of the repressor function of PNR, clear upregulation of Cyclin D1 and TBX2 gene expression was observed in the developing retina of mice that lacked functional PNR (rd7/rd7, a spontaneous PNR gene mutant line) (Figure 6B). However, in the retina of adult rd7/rd7 mice, upregulation of the TBX gene, but not the cyclin D1 gene, was observed, which suggested a developmental stage-specific function for PNR through interaction with multiple co-repressor complexes in the retina (see Figure 7). Indeed, by *in vivo* ChIP analysis, a clear Ret-CoR recruitment to the Cyclin D1 gene promoters was detected in the developing retina of P0 mice, rather than in the mature retina of adult mice (Figure 6C). As previously reported in mice and human ESCS patients (Akhmedov *et al*, 2000; Gerber *et al*, 2000; Haider *et al*, 2000), an increased number of S-cone cells with normal M-cone cell number was reported from the retina of rd7/rd7 mice (see upper panel in Figure 6D). In the retina of the wild-type mice at P0, S-cone opsin (stained as red) expression was not detected in the layers of PCNA-positive dividing cells (green), confirming that at P0 stage, no proliferation of the S-cone progenitor cells. However, in the retina of rd7/rd7 mice, S-cone opsin expression was detectable in the layers of PCNA-positive dividing cells (see arrowheads in lower panels in Figure 6D), suggesting that S-cone progenitor cells are still proliferating at P0. Such PNR function in retina development was then examined in embryonic retina cells (Figure 6E). Knockdown of PNR with a retrovirus (Supplementary Figure 1B) appeared to induce cell proliferation, as seen in hyperproliferative retina cells derived from rd7/rd7 mice at P0, supporting the putative PNR suppressive function for retina cell proliferation. Thus, Ret-CoR co-repressor function, presumably as an HDAC complex, appears to be required for PNR function in retinal progenitor cells, but not in differentiated retinal cells (Figure 7).

Discussion

The role of Ret-CoR function in retina development

PNR is known to serve as a negative regulator for cell proliferation of retina neurons. As established in ESCS patients and rd7/rd7 mice, S-cone cell proliferation appears under a negative control by PNR, whereas differentiation switching of S-cone cells into M-cone cells appears to require the other factors (Haider *et al*, 2001; Milam *et al*, 2002; Yanagi *et al*, 2002). The molecular mechanism of suppression of S-cone cell proliferation by PNR still remains elusive, but PNR-mediated transcriptional repression of genes involving cell-cycle regulation has been already revealed (Yanagi *et al*, 2002). Together with the present findings that the Ret-CoR

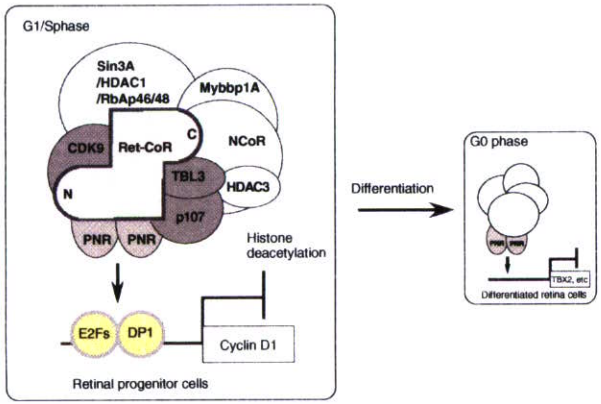

Figure 7 Schematic diagrams of PNR and Ret-CoR complex function. In the proliferative stage cells such as retinal progenitor cells, PNR is recruited together with a Ret-CoR containing complex on their target gene promoters at G1/S phase and inhibitory for cell proliferation. After cell differentiation, PNR with the other co-repressor complex(es) may control the target genes at G0 phase.

gene expresses in developing, but not in differentiated retina, Ret-CoR appears physiologically important for the PNR suppressor function for cell cycle regulation in retinal progenitor cells (Figure 7). Through the PNR-mediated transcriptional controls, Ret-CoR may serve as a suppressor for S-cone cell proliferation. Given the facts that Ret-CoR expression was also seen in brain, it is also possible to speculate that Ret-CoR co-represses the function of the other sequence-specific regulators, which determine cell fate of neurons through transcriptional control. In this respect, it is interesting to examine functional interaction of Ret-CoR with TLX and its relevance to physiological events in brain by comparing with the reported co-repressors (Perissi and Rosenfeld, 2005), although in the tested promoters of PNR and TLX target genes, Ret-CoR appeared unlikely to functionally associate with TLX.

Multiple co-repressor complexes facilitate the transrepressive function of PNR?

Transcriptional regulation by sequence-specific regulators upon the target gene promoters is believed to couple with histone modification and chromatin remodeling (McKenna and O'Malley, 2002; Belandia and Parker, 2003; Kitagawa *et al*, 2003; Perissi and Rosenfeld, 2005). Reflecting the biological events on the chromatin, a number of co-regulator complexes for NRs has been recently suggested to support the complicated but sequential cycling events for transcriptional events (Metivier *et al*, 2003). In this regard, it is reasonable to speculate that PNR requires multiple co-repressor complexes for its transrepressive function.

In retinal progenitor cells, we presume that the Ret-CoR HDAC complex co-represses PNR as a major co-repressor complex. However, from the findings that clear recruitment of Ret-CoR to the TBX2 gene promoter was undetectable, irrespective of the PNR-transrepressive function, in the differentiated retina of mice (Figure 6C), PNR appears to associate with the other HDAC complex(es) in differentiated retina cells. In fact, by a ChIP analysis of the TBX2 gene promoter in Y79 cells, a recruitment of HDAC1 without Ret-CoR was seen (Figure 5F). Together with the observations that Ret-CoR was absent on the TBX2 promoter in mouse retina (Figure 6C), PNR may associate with the other co-repressor complex(es), at least, in differentiated retina cells (Figure 7).

The cell cycle-dependent appearance of Ret-CoR is regulated through protein degradation?

Our findings suggested that the Ret-CoR complex acts as a negative regulatory complex of the cell cycle through inhibition of cell cycle-related factor gene expression via increased Ret-CoR protein levels during the G1/S transition stage. Supporting the cell cycle-dependent appearance of Ret-CoR protein, in the Ret-CoR harbors a destruction box R (1142)-R-A-L-G-R-M-V-E (1150) (compared to the consensus R-X-X-L-X-X-X-X-N/D/E) (Glotzer *et al*, 1991) identified in cyclin B as an interacting domain for E3 ligase and for cell cycle-regulated protein degradation (Wei *et al*, 2004). Consistently, Ret-CoR was highly susceptible to ubiquitination (Figure 3C), perhaps appearance of Ret-CoR protein is, at least in part, attributed to regulated protein degradation through the ubiquitin-dependent proteasomal pathway (Vodermaier, 2004; Peters, 2006). As endogenous Ret-CoR protein expression appears to be tightly regulated via the cell cycle, Ret-CoR function in the developing retina may be specific to late G1 stage or the G1/S transition stage, presumably in retinal progenitor cells. It is possible that through the co-regulatory function of such cell cycle-dependent co-repressor complexes, retina cell differentiation can be tightly regulated by PNR, along with other classes of sequence-specific regulators such as TRβ2 (Ng *et al*, 2001) and Crx (Furukawa *et al*, 1997), which together may constitute a photoreceptor-specific transcription factor cascade (Kobayashi *et al*, 1999; Gerber *et al*, 2000; Haider *et al*, 2000; Yanagi *et al*, 2002). In tissues that do not express PNR, such as the brain, cell cycle-dependent Ret-CoR complexes may also serve as co-repressor complexes for other sequence-specific regulators such as TLX. Although it remains unclear whether the functions of other known co-regulator complexes are also cell cycle-dependent, our findings suggest a model in which the level of expression of a co-regulator complex is regulated in a cell cycle-dependent manner.

Materials and methods

Purification and characterization of the Ret-CoR complex

Nuclear extracts (Yanagisawa *et al*, 2002; Kitagawa *et al*, 2003) from 293F cells transformed with Ret-CoR and Y79 cells with PNR were loaded onto an anti-FLAG M2 affinity resin column, and washed extensively with washing buffer (20 mM Tris–HCl (pH 8.0), 300 mM KCl, 0.2 mM EDTA, 0.05% NP40, 10% glycerol, 0.5 mM PMSF and 1 mM DTT). Bound proteins were eluted from the column by incubation with 133 μg/ml FLAG peptide in washing buffer for 30 min at room temperature. Next, the eluted solution was applied on the Protino column (MACHEREY-NAGEL) for His-tag binding and washed with a buffer His (40 mM HEPES pH 7.4, 300 mM KCl, 0.05% NP40, 10% glycerol). Ret-CoR complex was eluted by 250 mM Imidazole buffer His. For fractionation on glycerol gradients, elutants were layered on top of 13 ml linear 10–40% glycerol gradients in washing buffer and centrifuged for 16 h at 4°C at 40 000 r.p.m. in a SW-40 rotor (Beckman, CA). After getting each fraction, Re-IP was carried out with anti-RbAp46 antibody for fraction 10–12. Protein standards used were ovalbumin (44 kDa), β-globulin (158 kDa) and thyroglobulin (667 kDa). Each samples were applied on NuPAGE Bis–Tris 4–12% gradient gel (Invitrogen). Identification of each component was performed following our past papers (Kitagawa *et al*, 2002, 2003; Yanagisawa *et al*, 2002) using Voyager DE-STR (Perspective Biosystems).

Cell-cycle analysis

Y79 cells were synchronized at G1/S phase (with thymidine) and at G2/M phase (with demecolcine), essentially as described in our previous report (Kitagawa *et al*, 2003). Briefly, for the G1/S arrest, cells were exposed for 24 h with 2.5 mM thymidine in RPMI medium supplemented with 3% serum. Nine hours after the drug release, cells were cultured again for 16 h in the presence of 2.5 mM thymidine. Cells were yielded approximately 70% G1/S population. For the G2/M phase arrest, cells synchronized at G1/S phase by thymidine were released by incubation for 9 h with RPMI medium with 10% serum, and were treated with 0.015 μg/ml demecolcine for 8 h, which yielded approximately 75% G2/M population.

In vitro transcription

In vitro transcription with chromatin template was performed according to the previous report (Kitagawa *et al*, 2003; An and Roeder, 2004) using histone octamers from HeLa cell (Fujiki *et al*, 2005). Template DNA pG$_5$ML was kindly provided by Dr Robert G Roeder. Recombinant GAL-PNR LBD was expressed by pET system (Novagen), and purified by Protino Ni column under denaturing condition. Then the protein was refolded in a native buffer (20 mM HEPES, pH 7.9, 100 mM KCl, 0.2 mM EDTA, 10% glycerol, 0.5 mM DTT, 0.5 mM PMSF). Co-repressor activity of the purified Ret-CoR complex for PNR was attenuated in the presence of 500 nM TSA.

HDAC assay

HDAC assay was performed using HDAC Fluorescent Activity Assay/Drug Discovery Kit (AK-500, BIOMOL) according to the manufacturer's instructions. Briefly, cell extracts prepared from Y79 cells in 24-well plate were immunoprecipitaed with antibodies indicated and incubated with the substrate at 30°C for 30 min. After incubation, the reaction was stopped and the fluorescence was analyzed by microplate reading fluorimeter (Perkin Elmer).

Retroviral production and infection

shPNR, shRet-CoR and shControl expressing retroviruses were produced using pSIREN and 293gp-2 cells (Clontech). shPNR (corresponded to nucleotides 757–781), shRet-CoR (corresponding to nucleotides 2384–2408) and shControl (LacZ from *Escherichia Coli*: corresponding to nucleotides 291–311) was inserted in the pSIREN vector. Retina primary culture cells were infected by incubating them with the virus and 5 μg/ml hexadimethrine bromide (Sigma) following the manufacture's protocol (Clontech).

Retinal culture and cell proliferation assay

Neural retinas were dissected from postnatal day 0 mice or 3-month-old mice and cultured as pellets. The culture medium was a 1:1 mixture of Dulbecco's modified Eagle's medium (with Glutamax) and Ham's F12 (Gibco), supplemented with 10% FBS, insulin (10 μg/ml) and transferine (100 μg/ml). The cells were cultured 3 days by replacing half of the medium in the dish with fresh medium and used in cell proliferation assay.

The cell proliferation assay by incorporation of BrdU was performed using BrdU labelling and detection kit III (Roche) according to the instruction manual. All values are mean ± s.d. of at least three independent experiments.

Supplementary data

Supplementary data are available at *The EMBO Journal* Online (http://www.embojournal.org).

Acknowledgements

We thank Mime Kobayashi, Junn Yanagisawa, Keiichi Nakayama, Takumi Kamura, Makoto Nakanishi and Masanori Hatakeyama for helpful discussion and plasmids; Takafumi Shimizu, Yoshiko Yogiashi, Satoko Ogawa, Ken Ishitani and Kimihiro Yoshimura for technical assistance; H Higuchi for manuscript preparation; Robert G Roeder for vectors; Toshiya Tanaka and Tatsuhiko Kodama for the anti-PNR antibody; the DNA Analysis Shop, Veterinary Medical Sciences/Animal Resource Sciences, Graduate School of Agricultural and Life Sciences of The University of Tokyo for use of the ABI PRISM 7000 facility; and Kazuhiko Nakayama, of Olympus, for fluorescence microscopy analysis. This work was supported in part by a grant-in-aid for priority areas from the Ministry of Education, Culture, Sports, Science and Technology (to SK).

References

Akhmedov NB, Piriev NI, Chang B, Rapoport AL, Hawes NL, Nishina PM, Nusinowitz S, Heckenlively JR, Roderick TH, Kozak CA, Danciger M, Davisson MT, Farber DB (2000) A deletion in a photoreceptor-specific nuclear receptor mRNA causes retinal degeneration in the rd7 mouse. *Proc Natl Acad Sci USA* **97:** 5551–5556

An W, Roeder RG (2004) Reconstitution and transcriptional analysis of chromatin *in vitro*. In *Chromatin and Chromatin Remodeling Enzymes*, Allis CD, Wu C (eds) Vol. 377, pp 460–474. : Amsterdam:Elsevier Academic Press

Belandia B, Parker MG (2003) Nuclear receptors: a rendezvous for chromatin remodeling factors. *Cell* **114:** 277–280

De Falco G, Bagella L, Claudio PP, De Luca A, Fu Y, Calabretta B, Sala A, Giordano A (2000) Physical interaction between CDK9 and B-Myb results in suppression of B-Myb gene autoregulation. *Oncogene* **19:** 373–379

Fan M, Rhee J, St-Pierre J, Handschin C, Puigserver P, Lin J, Jaeger S, Erdjument-Bromage H, Tempst P, Spiegelman BM (2004) Suppression of mitochondrial respiration through recruitment of p160 myb binding protein to PGC-1alpha: modulation by p38 MAPK. *Genes Dev* **18:** 278–289

Fondell JD, Ge H, Roeder RG (1996) Ligand induction of a transcriptionally active thyroid hormone receptor coactivator complex. *Proc Natl Acad Sci USA* **93:** 8329–8333

Fujiki R, Kim MS, Sasaki Y, Yoshimura K, Kitagawa H, Kato S (2005) Ligand-induced transrepression by VDR through association of WSTF with acetylated histones. *EMBO J* **24:** 3881–3894

Furukawa T, Morrow EM, Cepko CL (1997) Crx, a novel otx-like homeobox gene, shows photoreceptor-specific expression and regulates photoreceptor differentiation. *Cell* **91:** 531–541

Gerber S, Rozet JM, Takezawa SI, dos Santos LC, Lopes L, Gribouval O, Penet C, Perrault I, Ducroq D, Souied E, Jeanpierre M, Romana

S, Frezal J, Ferraz F, Yu-Umesono R, Munnich A, Kaplan J (2000) The photoreceptor cell-specific nuclear receptor gene (PNR) accounts for retinitis pigmentosa in the Crypto-Jews from Portugal (Marranos), survivors from the Spanish Inquisition. *Hum Genet* **107:** 276–284

Glotzer M, Murray AW, Kirschner MW (1991) Cyclin is degraded by the ubiquitin pathway. *Nature* **349:** 132–138

Guenther MG, Lane WS, Fischle W, Verdin E, Lazar MA, Shiekhattar R (2000) A core SMRT corepressor complex containing HDAC3 and TBL1, a WD40-repeat protein linked to deafness. *Genes Dev* **14:** 1048–1057

Haider NB, Jacobson SG, Cideciyan AV, Swiderski R, Streb LM, Searby C, Beck G, Hockey R, Hanna DB, Gorman S, Duhl D, Carmi R, Bennett J, Weleber RG, Fishman GA, Wright AF, Stone EM, Sheffield VC (2000) Mutation of a nuclear receptor gene, NR2E3, causes enhanced S cone syndrome, a disorder of retinal cell fate. *Nat Genet* **24:** 127–131

Haider NB, Naggert JK, Nishina PM (2001) Excess cone cell proliferation due to lack of a functional NR2E3 causes retinal dysplasia and degeneration in rd7/rd7 mice. *Hum Mol Genet* **10:** 1619–1626

Heinzel T, Lavinsky RM, Mullen TM, Soderstrom M, Laherty CD, Torchia J, Yang WM, Brard G, Ngo SD, Davie JR, Seto E, Eisenman RN, Rose DW, Glass CK, Rosenfeld MG (1997) A complex containing N-CoR, mSin3 and histone deacetylase mediates transcriptional repression. *Nature* **387:** 43–48

Hu X, Lazar MA (1999) The CoRNR motif controls the recruitment of corepressors by nuclear hormone receptors. *Nature* **402:** 93–96

Kamei Y, Xu L, Heinzel T, Torchia J, Kurokawa R, Gloss B, Lin SC, Heyman RA, Rose DW, Glass CK, Rosenfeld MG (1996) A CBP integrator complex mediates transcriptional activation and AP-1 inhibition by nuclear receptors. *Cell* **85:** 403–414

Kitagawa H, Fujiki R, Yoshimura K, Mezaki Y, Uematsu Y, Matsui D, Ogawa S, Unno K, Okubo M, Tokita A, Nakagawa T, Ito T, Ishimi Y, Nagasawa H, Matsumoto T, Yanagisawa J, Kato S (2003) The chromatin-remodeling complex WINAC targets a nuclear receptor to promoters and is impaired in Williams syndrome. *Cell* **113:** 905–917

Kitagawa H, Yanagisawa J, Fuse H, Ogawa S, Yogiashi Y, Okuno A, Nagasawa H, Nakajima T, Matsumoto T, Kato S (2002) Ligand-selective potentiation of rat mineralocorticoid receptor activation function 1 by a CBP-containing histone acetyltransferase complex. *Mol Cell Biol* **22:** 3698–3706

Kobayashi M, Takezawa S, Hara K, Yu RT, Umesono Y, Agata K, Taniwaki M, Yasuda K, Umesono K (1999) Identification of a photoreceptor cell-specific nuclear receptor. *Proc Natl Acad Sci USA* **96:** 4814–4819

Li X, McDonnell DP (2002) The transcription factor B-Myb is maintained in an inhibited state in target cells through its interaction with the nuclear corepressors N-CoR and SMRT. *Mol Cell Biol* **22:** 3663–3673

Luo RX, Postigo AA, Dean DC (1998) Rb interacts with histone deacetylase to repress transcription. *Cell* **92:** 463–473

Mangelsdorf DJ, Thummel C, Beato M, Herrlich P, Schutz G, Umesono K, Blumberg B, Kastner P, Mark M, Chambon P, Evans RM (1995) The nuclear receptor superfamily: the second decade. *Cell* **83:** 835–839

McKenna NJ, O'Malley BW (2002) Combinatorial control of gene expression by nuclear receptors and coregulators. *Cell* **108:** 465–474

Metivier R, Penot G, Hubner MR, Reid G, Brand H, Kos M, Gannon F (2003) Estrogen receptor-alpha directs ordered, cyclical, and combinatorial recruitment of cofactors on a natural target promoter. *Cell* **115:** 751–763

Metzger E, Wissmann M, Yin N, Muller JM, Schneider R, Peters AH, Gunther T, Buettner R, Schule R (2005) LSD1 demethylates repressive histone marks to promote androgen-receptor-dependent transcription. *Nature* **437:** 436–439

Milam AH, Rose L, Cideciyan AV, Barakat MR, Tang WX, Gupta N, Aleman TS, Wright AF, Stone EM, Sheffield VC, Jacobson SG (2002) The nuclear receptor NR2E3 plays a role in human retinal photoreceptor differentiation and degeneration. *Proc Natl Acad Sci USA* **99:** 473–478

Nagase T, Ishikawa K, Suyama M, Kikuno R, Hirosawa M, Miyajima N, Tanaka A, Kotani H, Nomura N, Ohara O (1998) Prediction of the coding sequences of unidentified human genes. XII. The complete sequences of 100 new cDNA clones from brain which code for large proteins *in vitro*. *DNA Res* **5:** 355–364

Nagy L, Kao HY, Chakravarti D, Lin RJ, Hassig CA, Ayer DE, Schreiber SL, Evans RM (1997) Nuclear receptor repression mediated by a complex containing SMRT, mSin3A, and histone deacetylase. *Cell* **89:** 373–380

Narlikar GJ, Fan HY, Kingston RE (2002) Cooperation between complexes that regulate chromatin structure and transcription. *Cell* **108:** 475–487

Ng L, Hurley JB, Dierks B, Srinivas M, Salto C, Vennstrom B, Reh TA, Forrest D (2001) A thyroid hormone receptor that is required for the development of green cone photoreceptors. *Nat Genet* **27:** 94–98

Oh IH, Reddy EP (1999) The myb gene family in cell growth, differentiation and apoptosis. *Oncogene* **18:** 3017–3033

Ohtani K, DeGregori J, Nevins JR (1995) Regulation of the cyclin E gene by transcription factor E2F1. *Proc Natl Acad Sci USA* **92:** 12146–12150

Onate SA, Tsai SY, Tsai MJ, O'Malley BW (1995) Sequence and characterization of a coactivator for the steroid hormone receptor superfamily. *Science* **270:** 1354–1357

Perissi V, Aggarwal A, Glass CK, Rose DW, Rosenfeld MG (2004) A corepressor/coactivator exchange complex required for transcriptional activation by nuclear receptors and other regulated transcription factors. *Cell* **116:** 511–526

Perissi V, Rosenfeld MG (2005) Controlling nuclear receptors: the circular logic of cofactor cycles. *Nat Rev Mol Cell Biol* **6:** 542–554

Peters JM (2006) The anaphase promoting complex/cyclosome: a machine designed to destroy. *Nat Rev Mol Cell Biol* **7:** 644–656

Qian J, Esumi N, Chen Y, Wang Q, Chowers I, Zack DJ (2005) Identification of regulatory targets of tissue-specific transcription factors: application to retina-specific gene regulation. *Nucleic Acids Res* **33:** 3479–3491

Rachez C, Lemon BD, Suldan Z, Bromleigh V, Gamble M, Naar AM, Erdjument-Bromage H, Tempst P, Freedman LP (1999) Ligand-dependent transcription activation by nuclear receptors requires the DRIP complex. *Nature* **398:** 824–828

Rosenfeld MG, Lunyak VV, Glass CK (2006) Sensors and signals: a coactivator/corepressor/epigenetic code for integrating signal-dependent programs of transcriptional response. *Genes Dev* **20:** 1405–1428

Sicinski P, Donaher JL, Parker SB, Li T, Fazeli A, Gardner H, Haslam SZ, Bronson RT, Elledge SJ, Weinberg RA (1995) Cyclin D1 provides a link between development and oncogenesis in the retina and breast. *Cell* **82:** 621–630

Sowden JC, Holt JK, Meins M, Smith HK, Bhattacharya SS (2001) Expression of *Drosophila* omb-related T-box genes in the developing human and mouse neural retina. *Invest Ophthalmol Vis Sci* **42:** 3095–3102

Tavner FJ, Simpson R, Tashiro S, Favier D, Jenkins NA, Gilbert DJ, Copeland NG, Macmillan EM, Lutwyche J, Keough RA, Ishii S, Gonda TJ (1998) Molecular cloning reveals that the p160 Myb-binding protein is a novel, predominantly nucleolar protein which may play a role in transactivation by Myb. *Mol Cell Biol* **18:** 989–1002

Vodermaier HC (2004) APC/C and SCF: controlling each other and the cell cycle. *Curr Biol* **14:** R787–R796

Wei W, Ayad NG, Wan Y, Zhang GJ, Kirschner MW, Kaelin Jr WG (2004) Degradation of the SCF component Skp2 in cell-cycle phase G1 by the anaphase-promoting complex. *Nature* **428:** 194–198

Weinstat-Saslow DL, Germino GG, Somlo S, Reeders ST (1993) A transducin-like gene maps to the autosomal dominant polycystic kidney disease gene region. *Genomics* **18:** 709–711

Yanagi Y, Takezawa S, Kato S (2002) Distinct functions of photoreceptor cell-specific nuclear receptor, thyroid hormone receptor beta2 and CRX in one photoreceptor development. *Invest Ophthalmol Vis Sci* **43:** 3489–3494

Yanagisawa J, Kitagawa H, Yanagida M, Wada O, Ogawa S, Nakagomi M, Oishi H, Yamamoto Y, Nagasawa H, McMahon SB, Cole MD, Tora L, Takahashi N, Kato S (2002) Nuclear receptor function requires a TFTC-type histone acetyl transferase complex. *Mol Cell* **9:** 553–562

Zhang CL, Zou Y, Yu RT, Gage FH, Evans RM (2006) Nuclear receptor TLX prevents retinal dystrophy and recruits the corepressor atrophin1. *Genes Dev* **20:** 1308–1320

MOLECULAR AND CELLULAR BIOLOGY, Nov. 2007, p. 7947–7954 Vol. 27, No. 22
0270-7306/07/$08.00+0 doi:10.1128/MCB.00813-07

Vitamin K Induces Osteoblast Differentiation through Pregnane X Receptor-Mediated Transcriptional Control of the Msx2 Gene[▽]

Mamoru Igarashi,[1] Yoshiko Yogiashi,[1,2] Masatomo Mihara,[1] Ichiro Takada,[1] Hirochika Kitagawa,[1] and Shigeaki Kato[1,2]*

The Institute of Molecular and Cellular Biosciences, The University of Tokyo, 1-1-1 Yayoi, Bunkyo-ku, Tokyo 113-0032, Japan,[1] and ERATO, Japan Science and Technology Agency, 4-1-8 Honcho, Kawaguchi, Saitama 332-0012, Japan[2]

Received 9 May 2007/Returned for modification 11 June 2007/Accepted 31 August 2007

Vitamin K is a fat-soluble vitamin that serves as a coenzyme for vitamin K-dependent carboxylase. Besides its canonical action, vitamin K binds to the steroid and xenobiotic receptor (SXR)/pregnane X receptor (PXR) and modulates gene transcription. To determine if the osteoprotective action of vitamin K is the result of the PXR/SXR pathway, we screened by two-dimensional sodium dodecyl sulfate-polyacrylamide gel electrophoresis the PXR/SXR target genes in an osteoblastic cell line (MC3T3-E1) treated with a vitamin K2 (menaquinone 4 [MK4]). Osteoblastic differentiation of MC3T3-E1 cells was induced by MK4. Msx2, an osteoblastogenic transcription factor, was identified as an MK4-induced gene. Functional analysis of the Msx2 gene promoter mapped a vitamin K-responsive element (PXR-responsive element [PXRE]) that was directly bound by a PXR/retinoid X receptor α heterodimer. In a chromatin immunoprecipitation analysis, PXR was recruited together with a coactivator, p300, to the PXRE in the Msx2 promoter. MK4-bound PXR cooperated with estrogen-bound estrogen receptor α to control transcription at the Msx2 promoter. Knockdown of either PXR or Msx2 attenuated the effect of MK4 on osteoblastic differentiation. Thus, the present study suggests that Msx2 is a target gene for PXR activated by vitamin K and suggests that the osteoprotective action of MK4 in the human mediates, at least in part, a genomic pathway of vitamin K signaling.

The K vitamins are a group of fat-soluble vitamins that occur in two natural forms: phyloquinones (K1) and menaquinones (K2). Vitamin K (VK) has classically been associated with blood coagulation (31). In its canonical role, VK serves as a coenzyme for VK-dependent carboxylase. This enzyme converts glutamate residues into γ-carboxyglutamate (Gla) residues in VK-dependent proteins, such as prothrombin, and factors IX and X (6, 10, 29). Such VK-induced protein modification also occurs in osteocalcin (7, 21) and matrix Gla protein (MGP) (22). Thus, VK may exert beneficial effects on bone formation and remodeling. In fact, animal studies suggest that VK deficiency results in a reduction in bone mass together with hypocarboxylation of osteocalcin (25).

Clinically, the most common form of K2, menaquinone 4 (MK4), has been shown to prevent bone fractures (3). This osteoprotective effect is more pronounced in K2 than in K1, and hence MK4 has been used to treat osteoporotic patients in Japan (9, 11, 28). However, the bone phenotypic abnormalities of mice deficient in osteocalcin and MGP do not fully support the classical view that the osteoprotective action of VK is the result of the modification of skeletal proteins. These mice, which are genetically deficient for osteocalcin or MGP, exhibited bone mass increases instead of losses (4). This suggests that the osteoprotective action of VK is mediated by another pathway.

MK4 recently has been shown to act as a ligand for the steroid and xenobiotic receptor (SXR) in human osteoblastic cells (33). It transcriptionally regulates gene expression and represents a new pathway of VK action. The SXR and its mouse homolog, the pregnane X receptor (PXR), respond to xenobiotics and pregnenones. PXR and SXR are members of the nuclear receptor (NR) gene superfamily and bind to specific DNA elements (PXR-responsive elements [PXRE]) as heterodimers with one of the retinoid X receptor (RXR) subtypes (α, β, and γ) (1, 2, 15, 16, 18). Like the other NR members, ligand binding to PXR/SXR induces dissociation of corepressors and recruitment of coactivators for ligand-induced transactivation in the target gene promoters (17). Thus, these findings suggest that it is feasible that the osteoprotective VK action mediates its transcriptional control of the VK target genes via PXR/SXR. In fact, several PXR/SXR genes recently have been shown to transcriptionally respond to VK (8).

To test this idea, we screened VK target genes in an osteoblastic cell line (MC3T3-E1) treated with MK4 with two-dimensional sodium dodecyl sulfate-polyacrylamide gel electrophoresis (2D SDS-PAGE). A prime osteoblastogenic factor, Msx2, was identified, and a PXRE was located in its gene promoter. MK4 interacted with the PXRE via PXR/RXRα binding in vivo and in vitro. Osteoblast genesis in MC3T3-E1 cells was induced by MK4, but knockdown of Msx2 by RNA interference (RNAi) abrogated the MK4 effect. The present study suggests that Msx2 is a target gene for VK-activated PXR/SXR. It implies that the osteoprotective VK action takes place, at least in part, on a genomic level by stimulating osteoblast differentiation through Msx2 gene induction.

* Corresponding author. Mailing address: The Institute of Molecular and Cellular Biosciences, The University of Tokyo, 1-1-1 Yayoi, Bunkyo-ku, Tokyo 113-0032, Japan. Phone: 81-3-5841-8478. Fax: 81-3-5841-8477. E-mail: uskato@mail.ecc.u-tokyo.ac.jp.

▽ Published ahead of print on 17 September 2007.

MATERIALS AND METHODS

Plasmids. The full-length cDNA for the mouse PXR (15) was subcloned into a pcDNA3 expression vector (Invitrogen) tagged with the hemagglutinin epitope